Dynamics of domain walls in weak ferromagnets

V. G. Bar'yakhtar, B. A. Ivanov, and M. V. Chetkin

Institute of Theoretical Physics, Academy of Sciences of the Ukrainian SSR, Kiev; T. G. Shevchenko State University, Kiev; M. V. Lomonosov State University, Moscow

Usp. Fiz. Nauk **146**, 417–458 (July 1985)

The up-to-date theoretical and experimental data on the fairly-high-velocity motion of a solitary domain wall in a weak ferromagnet are reviewed. The experimental data pertain to orthorhombic and uniaxial crystals of the orthoferrite and iron-borate types. The theoretical analysis demonstrates the great generality of the nonlinear dynamics of walls in weak ferromagnets of different symmetries. The necessary data on the magnetic structure and the magneto-optical properties of weak ferromagnets are presented. The experimental techniques of investigating domain-wall motion, including non-steady-state motion, are described. Mobility and limiting-wall-velocity data are given, and a quantitative theoretical description of these experiments is presented. The magnetoelastic anomalies observed experimentally in the case when the wall velocity is close to the velocity of sound are described. A theory of this phenomenon is given which is based on the notion of Cherenkov emission of sound by a moving wall. The results of the investigation of the non-steady-state and nonlinear domain-wall motion that arises due to an instability of the wall front are presented, and theoretical models are proposed for such motion.

CONTENTS

INTRODUCTION

The physical properties of real magnetically ordered substances are to a large extent determined by the existence of a domain structure.[1] The main ideas about domain structure and the properties of domain walls (DW) were developed in the pioneering papers of Weiss,[2] Bloch,[3] Landau and Lifshitz,[7] and Néel.[5] The experimental proof of the existence of domains, and the clarification of their role in the magnetization of ferromagnets were accomplished in the classic experiments of Barkhausen,[6] Bitter,[7], Akulov and Dekhtyar,[8] and Sixtus and Tonks.[9] The detailed investigation of domains and DW was held up for a long time by the absence of high-grade magnetically ordered crystals (referred to below as magnetic materials) and the complexity of the domain structure of bulk samples. The situation changed significantly in the 1960's, after the production of perfect ferrodielectric single crystals, especially single crystals in the form of thin films and platelets. The progress made in the study of domains in such samples is largely due to the production of optically transparent magnetic materials (see Ref. 10). Modern experimental methods (first and foremost the magneto-optical methods) allow a detailed investigation of the static and dynamic properties of individual DW's or of a solitary domain.

The possibility that domains (especially cylindrical magnetic domains or bubbles) could be used to fabricate components for modern computers drew the attention of a large number of researchers to this problem, generating a "bubble boom" (see Refs. 11 and 12). On the other hand, the elegance of the relationships that were established in the course of the investigation aroused the interest in this field of physicists engaged in fundamental research. Moving DW and domains in the theoretical description are, in fact, nonlinear solitary magnetization waves (magnetic solitons). The soliton concept is a new and extremely fruitful concept of modern theoretical and mathematical physics.[13] It turned out that domain and DW dynamics can be most adequately

 0038-5670/85/070563-26$01.80

described on the basis of soliton theory.[14] The large amount of data accumulated in the experimental investigation of DW dynamics is an important basis for the development of soliton theory. The indicated facts make the investigation of nonlinear DW dynamics timely both from the point of view of application and for progress in the fundamental investigations of magnetic substances.

Thus far, domain dynamics has been most thoroughly investigated for two classes of magnetically ordered crystals[1)]: The ferrite-garnets and the rare-earth orthoferrites. Notice that it is just these crystals that were the first-known transparent magnetic materials.[10] These two classes of magnetic substances differ essentially in both their macroscopic and dynamic properties. The ferrite-garnets are typical uncompensated ferrimagnets, and, from the macroscopic point of view, behave like ferromagnets. The rare-earth orthoferrites are an example of the so-called weak ferromagnets (WFM). These materials are similar to antiferromagnets, i.e., the magnetic moments of the sublattices in them are almost fully compensated. The spontaneous magnetic moment of a WFM (in partiuclar, of the orthoferrites) is extremely small, and is due only to a slight Dzyaloshinskiĭ-interaction-induced noncollinearity of the sublattice magnetic moments[15] (see also Refs. 16 and 17). As a result, the energy associated with the demagnetizing fields in a WFM is significantly (two-to-three orders of magnitude) smaller than the characteristic energy of the other relativistic interactions (e.g., the magnetic-anisotropy energy). Analysis shows that this essentially distinguishes their static and, especially, dynamic properties from the properties of the ferrite-garnets, in which the corresponding quantities are of the same order of magnitude, or differ by an order of magnitude.

The nonlinear dynamics of magnetic materials is described on the basis of the Landau-Lifshitz equation[4] (see also Refs. 16–18) for the sublattice magnetization vectors. For the ferrite-garnets the effective-ferromagnet approximation, according to which the ferrite is described by an equation for the resultant magnetization,[2)] is a good one. These equations have been solved for the fairly-high-velocity motion of a plane DW that is homogeneous in its own plane in both the cases of a uniaxial[20] and an orthorhombic ferromagnet,[21] the solution being customarily called the Walker solution. This solution is characterized by the fact that, according to it, the velocity of the translational motion of a DW cannot exceed a certain limiting value, called the Walker limit.

But the results of experimental investigations of DW motion in the ferrite-garnets disagree significantly with the theory constructed on the basis of the Walker solution. In particular, the value of the limiting velocity can be significantly smaller than the Walker limit, the dependence of the velocity of the forced motion of a wall on the driving force is different, etc.[12] This disagreement has been analyzed by a number of authors (see Ref. 12). It turns out that it is due to the fact that, in the ferrite-garnets, a DW is practically always not homogeneous in its own plane. Moreover, there begins to occur during the motion of a DW with a velocity significantly lower than the Walker limit a dynamic reconstruction of the DW inhomogeneities that exerts the dominant influence on the DW dynamics. It has not been established that such a complicated DW-motion picture in the ferrite-garnets is due to the effect of the long-range demagnetizing fields. The problem of allowing for these fields is an extremely complicated one, since the one-dimensional nonlinear Landau-Lifshitz differential equation then becomes a non-unidimensional integrodifferential equation. Notwithstanding the number of advances made in the theoretical description of certain aspects of DW dynamics,[12] there is at present no quantitative theory that allows us to describe fully DW motion in magnetic materials of the ferrite-garnet type.[3)]

The situation is significantly different in the case of WFM. The experimental investigations of the orthoferrites, which were begun in the 1970's, have shown that the DW's in the orthoferrites can move with very high velocities (for greater details, see Sec. 2). For a long time these results also could not be explained on the basis of the Walker solution. In particular, it was noted that the limiting value of the velocity is significantly greater (and not smaller, as in the case of the ferrite-garnets) than the Walker limit. But this disagreement was cleared up at the end of the 1970's, when it was noted that the direct use of the Walker solution is incorrect, since it ignores the sublattice structure of the WFM. After this fact had been realized, and a theory based on a two-sublattice model had been constructed, it was found that the simple one-dimensional model (which ignores the inhomogeneities in the plane of the wall) explains very well the main aspects of DW dynamics in the orthoferrites (see Sec. 3 below).

This is due to an extremely propitious situation, about which we have already spoken: the demagnetizing-field-related nonlocal interaction in a WFM is extremely weak, and does not have a significant effect on the DW dynamics.

The measured external-field dependence of the velocity exhibits anomalies at values of the velocity close to the values of the longitudinal and transverse sound velocities. These anomalies can be explained as being a consequence of Cherenkov emission of phonons (see Sec. 4).

Recently it was found that the DW motion can become highly nonstationary at high velocities. These results are discussed in Sec. 5.

Recent investigations of DW motion in iron borate—an easy-plane WFM—have demonstrated that the principal laws governing DW dynamics in WFM's with different types of magnetic anisotropy are basically similar, and are well described by the existing theory.

Thus, at present the study of nonlinear DW dynamics in the WFM's has advanced considerably further than the study of the phenomenon in any other magnetic materials, e.g., materials of the ferrite-garnet type. The existence of precision measurement techniques allows us to investigate a number of fine effects with a high degree of accuracy. On the other hand, we have an adequate theoretical description of these effects, which, as a rule, agrees quantitatively with experiment. The above-outlined range of problems constitutes an integral and extremely important section of the nonlinear physics of magnetism, the development of which is essential

to both fundamental and applied physics.

It is these facts that prompted the authors to write the present review. We hope that the systematic exposition of the results obtained in the investigation of nonlinear DW dynamics in the WFM's will facilitate further development of domain dynamics research as an important section of the modern physics of magnetism.

1. MAGNETIC STRUCTURE AND MAGNETO-OPTICAL PROPERTIES OF THE ORTHOFERRITES

a) The free energy and structure of domain walls

The rare-earth orthoferrites, with general formula $RFeO_3$ (where R is an ion of the rare-earth elements) and crystal symmetry group D_{2h}^{16}, form a large class of weakly magnetic antiferromagnets that is presently being intensively studied, and is the object of our review. Single crystals of the orthoferrites are obtained by the methods of spontaneous crystallization from a solution in the melt,[22] hydrothermal synthesis,[33] and crucibleless zone refining with optical heating,[24] the last methods giving the largest and optically the most transparent crystals. Below we discuss those properties of the orthoferrites which are necessary for the present review. More comprehensive experimental and theoretical data on them can be found in Ref. 25.

We shall describe an orthoferrite as a WFM with two magnetic sublattices whose magnetizations are equal to $\mathbf{M}_1$ and $\mathbf{M}_2$. It is convenient to introduce the normalized magnetization and antiferromagnetism vectors, $\mathbf{m}$ and $\mathbf{l}$ respectively, defined as

$$\mathbf{m}=\frac{\mathbf{M}_1+\mathbf{M}_2}{2M_0}, \qquad \mathbf{l}=\frac{\mathbf{M}_1-\mathbf{M}_2}{2M_0}. \tag{1.1}$$

On account of the constancy of the lengths of the sublattice moments ($\mathbf{M}_1^2=\mathbf{M}_2^2=\mathbf{M}_0^2$), the vectors $\mathbf{m}$ and $\mathbf{l}$ are connected by the relation

$$\mathbf{ml}=0, \quad \mathbf{m}^2+\mathbf{l}^2=1. \tag{1.2}$$

Let us write the energy density of the WFM in the form

$$w=M_0^2\left(\frac{1}{2}\delta\mathbf{m}^2+\frac{1}{2}\sum_{i,\,k=1}^{3}\alpha_{ik}\frac{\partial\mathbf{l}}{\partial x_i}\frac{\partial\mathbf{l}}{\partial x_k}+w_a^{(0)}+w_{\mathbf{D}}-2\mathbf{mh}\right). \tag{1.3}$$

Here α_{ik} and δ are respectively the inhomogeneous and homogeneous exchange constants ($\delta\sim T_{\mathrm{N}}/\mu_0 M_0$ and $\alpha\sim\delta a^2$, where T_{N} is the Néel temperature and a is the lattice constant) and $\mathbf{h}=\mathbf{H}/M_0$, $\mathbf{H}$ being the external field. The forms of the anisotropy energy $w_a^{(0)}$ and the Dzyaloshinskiĭ interaction energy $w_{\mathbf{D}}$ are determined by the symmetry of the WFM. In a uniaxial WFM with an even principal axis

$$w_{\mathbf{D}}=\mathbf{d}\,[\mathbf{ml}], \tag{1.4}$$

where $\mathbf{d}$ is a vector oriented along the principal axis and the quantity $dM_0/2$ is equal to the Dzyaloshinskiĭ field H_{D}. We can use this formula in the description of the orthoferrites if we consider $\mathbf{d}$ to be oriented along the b axis.

In writing down (1.3) we took into account the fact that, in sufficiently weak fields (i.e., that for $h\ll\delta$), $\mathbf{m}^2\ll\mathbf{l}^2\approx 1$. Therefore, in (1.3) we have dropped the terms with $(\nabla\mathbf{m})^2$, and can ignore the dependence of $w_a^{(0)}$ on the components of $\mathbf{m}$. In this case it is easy to express $\mathbf{m}$ in terms of the components of $\mathbf{l}$. Minimizing (1.3) with allowance for (1.2) and (1.4), we obtain

$$\mathbf{m}=\frac{1}{\delta}\{[\mathbf{dl}]+2(\mathbf{h}-\mathbf{l}(\mathbf{hl}))\}. \tag{1.5}$$

With allowance for (1.5), the energy of the WFM expressed in terms of the unit vector $\mathbf{l}$ ($\mathbf{l}^2=1$) assumes the form

$$W=M_0^2\int \mathrm{d}\mathbf{r}\left\{\frac{1}{2}\alpha(\nabla\mathbf{l})^2+w_a+\frac{2}{\delta}(\mathbf{lh})^2+\frac{2}{\delta}\mathbf{l}\,[\mathbf{hd}]\right\}. \tag{1.6}$$

Here we have set $\alpha_{ik}=\alpha\delta_{ik}$, which holds for the orthoferrites with a high degree of accuracy, and $w_a=w_a^{(0)}+(\mathbf{dl})^2/2\delta$ is the effective anisotropy energy. It is clear that the stucture of w_a is the same as that of $w_a^{(0)}$, and that it is determined by the symmetry of the WFM. For an orthoferrite

$$w_a=\frac{1}{2}(\beta_1 l_z^2+\beta_2 l_y^2). \tag{1.7}$$

We shall assume that the x, y, z axes coincide wth the crystal axes a, b, c. As experiment shows[26] (see also Ref. 25), at high temperatures the vectors $\mathbf{l}$ and $\mathbf{m}$ in all the orthoferrites are oriented along the a and c axes respectively. As the temperature is lowered, there occurs in some of the orthoferrites a reorientation of $\mathbf{l}$ and $\mathbf{m}$; this reorientation is described by the dependence of the constants β_1 and β_2 on the temperature. The high-temperature phase $\Phi_{\parallel}$ is stable when $\beta_1(T)>0$ and $\beta_2(T)>0$. If $\beta_1(T)$ changes sign, then there occurs a transition into the low-temperature weakly-ferromagnetic phase $\Phi_{\perp}$; in the process the vector $\mathbf{l}$ realigns itself along the c axis, while the vector $\mathbf{m}$ realigns itself along the a axis. Such a transition occurs in $SmFeO_3$, $TmFeO_3$, and other orthoferrites. If, on the other hand, $\beta_2(T)$ changes sign, then the orthoferrite goes over into the antiferromagnetic state ($\mathbf{l}$ is parallel to the $\mathbf{b}$ axis and $m=0$). Such a transition occurs in $DyFeO_3$. The DW's in the reorientation region have a number of special features.[27,28]

The above-described homogeneous states are twofold degenerate: the state with $\mathbf{l}_0$, $\mathbf{m}_0$ and the one with $-\mathbf{l}_0$, $-\mathbf{m}_0$ correspond to the same energy. This leads to the occurrence of 180-degree domain walls (DW). Let us consider the structure of the DW in the $\Phi_{\parallel}$ phase.

It is convenient to go over to the angle variables for the unit vector $\mathbf{l}$:

$$l_x=\cos\theta, \quad l_y=\sin\theta\sin\varphi, \quad l_z=\sin\theta\cos\varphi. \tag{1.8}$$

To the $\Phi_{\parallel}$ phase corresponds $\mathbf{l}\parallel\mathbf{a}$, i.e., the values $\theta=0$, π. Analysis shows that two types of DW can exist in an orthorhombic WFM. To one of them (the ac-type wall) corresponds the value $\varphi=0$, i.e, an $\mathbf{l}$ rotation in the (x,y) plane. To the other corresponds a wall of the type of an ab-rotation of $\mathbf{l}$ in the (x,y) plane ($\varphi=\pi/2$). The distribution of the angle θ in both DW is given by the equation

$$\alpha\frac{\mathrm{d}^2\theta}{\mathrm{d}\xi^2}-\beta\sin\theta\cos\theta=0, \tag{1.9}$$

where $\beta=\beta_1$ and β_2 for the ac- and ab-type walls respec-

tively and ξ is the coordinate along the axis normal to the DW surface.

The solution to this equation with the boundary conditions $\theta(-\infty)=\pi$ and $\theta(+\infty)=0$ describes both types of DW, and has the form

$$\operatorname{tg}\frac{\theta}{2}=\exp\left(-\frac{\xi}{x_{0i}}\right),\quad x_{0i}=\sqrt{\frac{\alpha}{\beta_i}}. \tag{1.10}$$

To these DW correspond significantly different magnetic-moment (**m**) distributions.[29] For the *ac*-type wall the vector **m**, like the vector **l**, rotates in the (*a*, *c*) plane with almost a constant length. In the *ab*-type wall the vector **m** is always oriented along the *z* axis, and varies only in magnitude.

The presence of two types of DW with the same **m** and **l** values at points far from a wall raises the question of stability of the walls. The point is that it turns out in the analysis of a DW as a topological soliton that, if to the wall correspond different values of **m** at $\xi\to+\infty$ and $\xi\to-\infty$, then the wall cannot, on the strength of topological arguments, be eliminated.[30] But topological considerations cannot exclude the instability of one of the two possible walls with respect to transformation into the other.[4)]

The analysis carried out in Ref. 27 shows that only one of the two DW, namely, the one to which corresponds the smaller energy (the lower value of the constant β_i), is stable. The second DW is absolutely unstable against weak perturbations (this can be seen from, for example, the formula (3.5) obtained below). Generally speaking, the constants β_1 and β_2 depend on the temperature differently. Consequently, if the difference $(\beta_1-\beta_2)$ changes sign at some temperature, one type of DW in the magnetic material should go over into a DW of the other type on going through this point. Such a transformation has been found to occur in dysprosium orthoferrite $DyFeO_3$ at $T=150$ °K (Ref. 32), with walls of the *ab* type occurring at temperatures below 150 °K and those of the *ac* type, at temperatures above this point. Notice that the moment reorientation in a DW is not the same as ordinary spin flip, which occurs upon the reversal of the sign of one of the constants β_i (the smaller one), and not their difference. In $DyFeO_3$ the spin flip (the Morin point) occurs, for example, at $T=40$ °K, i.e., at a temperature significantly lower than the temperature at which the transformation of the *ac*-type walls into *ab*-type ones occurs. In our opinion, it is of interest to study the dynamic properties of the DW in the vicinity of this transition.

The *ac*-type walls with different orientations can be divided into the following classes: quasi-Bloch walls (the vector **m** rotates in the plane of the DW), quasi-Néel walls (the vector **m** is perpendicular to the DW plane), and the so-called head-to-head walls. To the last class corresponds a nonzero jump in the magnetization, i.e., a head-to-head wall is charged, and produces a demagnetizing field at points far from itself. In an *ab*-type wall the vector **m** does not rotate, and such a classification does not apply. Since the energy associated with the demagnetizing fields in the orthoferrites is small, the energies of these DW are close to each other, but their dynamic properties differ somewhat. The difference between these DW manifests itself especially strongly when allowance is made for the magnetoelastic interactions (see Secs. 2 and 3 below).

As we shall show in Sec. 3, this classification of the DW and their structural characteristics holds true in the analysis of the moving DW.

b) Optical and magneto-optical properties

The progress that has been made in the study of the domains in the orthoferrites is essentially connected with the application of optical methods of detection of domain structures. This is particularly manifest in the investigation of DW dynamics. The techniques of double-shot high-speed photography, bubble collapse, and measurement of the time of travel by a DW of a given distance between two light spots are based on the use of the phenomenon of optical transparency and the Faraday effect. As we have already noted, the weakly ferromagnetic orthoferrites, together with the ferrite-garnets, were the first-known optically transparent magnetic materials.[33,10] They are transparent in the infrared region of the spectrum; in the 1.1–6 μm wavelength region the absorption coefficient does not exceed a few tenths of a cm^{-1}. The orthoferrites, unlike the ferrite-garnets, possess a sufficiently high transmittance in the visible region of the spectrum as well. This is largely due to the fact that the iron ions enter into the orthoferrite lattice in only one octahedral coordination. The results of a calculation of the splitting of the Fe^{3+}-ion levels by the crystal field are given in Ref. 10. Figure 1 shows the coefficients of absorption of light of the visible and infrared regions of the spectrum in $ErFeO_3$.[34] The region of high transparency of the orthoferrites lies in the vicinity of the wave-lengths 0.63 μm. The minimum absorption coefficient at this wavelength is about 150 cm^{-1}. The two broad absorption bands in the region extending from 0.7 to 1 μm correspond to the ${}^6A_{1g}\to{}^4T_{1g}$ and ${}^6A_{1g}\to{}^4T_{2g}$ transitions in the Er^{3+} ions. At wavelengths greater than 8 μm, we have a much more intense absorption, which is brought about by the lattice vibrations lying in the 1300–1600 cm^{-1} spectral region. The transmission spectra of the orthoferrites of Tb, Ho, Tm, Er, and Yb in the far infrared region have been investigated by Smith *et al.*[35] Figure 2 shows the spectral dependence of the transmittance of

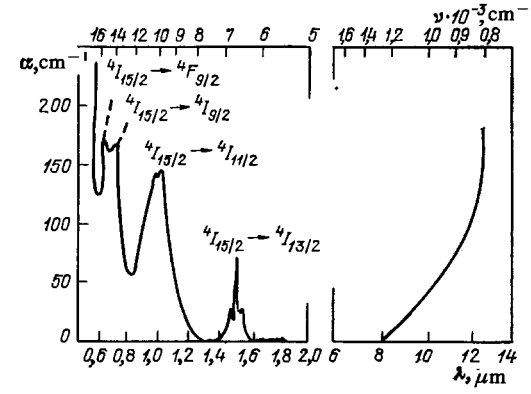

FIG. 1. Coefficient of absorption of light in erbium orthoferrite in the visible and infrared regions.[34]

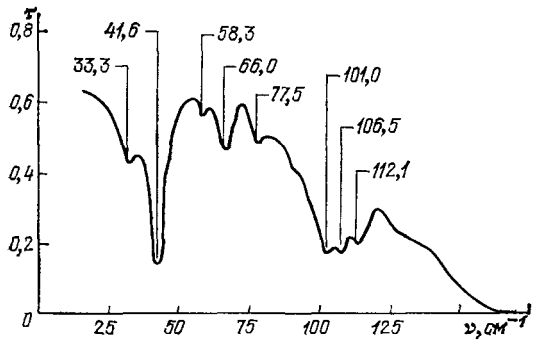

FIG. 2. Transmission spectrum of thulium orthoferrite in the far infrared region.[35]

$TmFeO_3$ at 4.2 °K. The absorption lines near 101.1 and 112.1 cm^{-1} occur in all the investigated orthoferrites, and are due to the optical phonons. The remaining absorption lines are due to electric dipole transitions between the principal-multiplet levels split by the crystal field.

As has been noted, the orthoferrites are orthorhombic crystals (with space group D_{2h}^{16}). They are optically biaxial, and are highly birefringent. Orthogonal, elliptically polarized waves are the normal types of electromagnetic waves that propagate in a longitudinally magnetized birefringent transparent crystal.[18] When two such waves propagating in a crystal with different velocities interfere as they come out of the crystal, an elliptically polarized wave is produced. The major axis of the ellipse is then inclined at an angle θ to the direction of the linear polarization of the wave incident on the crystal. For an incident wave polarized along the crystallographic axes perpendicular to the direction of the weak ferromagnetism,

$$\operatorname{tg} 2\theta = \frac{2\gamma}{n_x^2 - n_y^2} \sin \frac{2\pi l (n_x - n_y)}{\lambda}; \qquad (1.11)$$

here $n_x = \sqrt{\varepsilon_{xx}}$, $n_y = \sqrt{\varepsilon_{yy}}$, $\gamma = i\varepsilon_{xy}$, λ is the wavelength of the light, and l is the plate thickness. The expression (1.11) was derived under the assumption that

$$| \varepsilon_{xx} - \varepsilon_{yy} | \gg | \gamma |, \qquad (1.12)$$

which holds well for the orthoferrites. It follows from (1.11) that θ is an oscillating function of λ, the amplitude of the oscillations being, on account of (1.12), small. The expression (1.11) goes over, when $n_x = n_y$, into the standard formula for the Faraday rotation angle[36]:

$$\theta = \frac{\pi \gamma l}{n\lambda}.$$

In Ref. 37 the expressions for the rotation angle θ and the ellipticity parameter are derived without the limitation (1.12) with the use of the Jones matrix method.

Figure 3 shows the spectral dependences $\theta(\lambda)$ at the exits of $YFeO_3$ samples of different thicknesses, cut perpendicular to the [001] axis (the *c* axis).[38]

In the infrared region, where the birefringence dispersion is small, we can determine the quantity $\Delta n = n_x - n_y$ from the two neighboring λ values at which $\theta(\lambda) = 0$. The Δn values obtained in this way for $YFeO_3$ in the 1.1–1.8 μm wavelength region ranged[38] from 3×10^{-2} to 4×10^{-2}, which agree with the data obtained later with the use of compensators.[39] In the visible region of the spectrum the birefringence dispersion in the orthoferrites is strong, and compensators were used to determine Δn. The results reported indicate that the birefringence of the orthoferrites substantially limits the angles of rotation of the polarization plane when light propagates along the axis of weak ferromagnetism. For light of wavelength 0.63 μm, at which the transmittance of the orthoferrites is fairly high, θ does not exceed 1.5–2°. This leads to a low optical contrast between the observed domain structures. the magnitudes of the off-diagonal elements of the ε_{ik} tensor for all the orthoferrites investigated to date[38–41] turn out to be unusually large. they are several times greater than the analogous quantities for the ferrite-garnets, and are not proportional to the small ferromagnetic moment. To explain the strong linear magnetooptical effects in the orthoferrites, several mechanisms have been proposed, the main idea of which consists in an attempt to relate them to the antiferromagnetism vector.[41,42]

The unusually large magnitudes of the off-diagonal elements of the ε_{ik} tensor for the orthoferrites stimulated the investigation in these crystals of the Faraday effect in the case of light propagating along the optic axis, where, according to (1.11), the effect of the birefringence on the quantity θ vanishes. Measurements of the principal refractive indices of a number of orthoferrites[39,43] have shown that the optic axes of these crystals lie in the (100) plane, and that at wave-

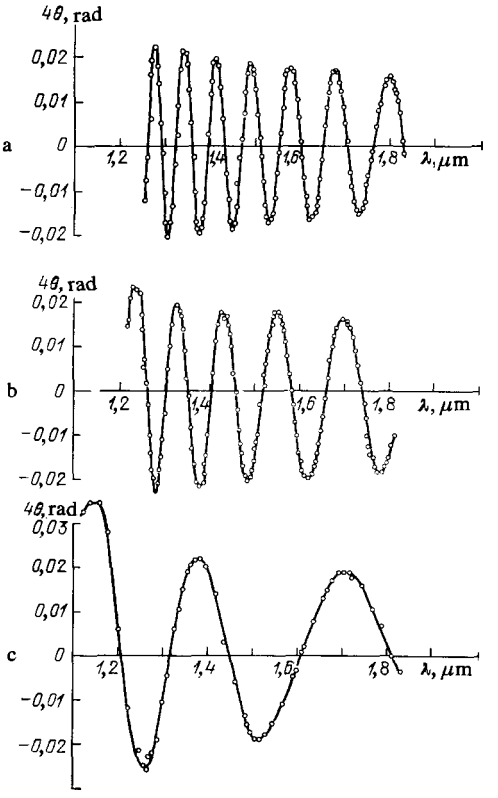

FIG. 3. Spectral dependence of the angle of rotation of the major axis of the polarization ellipse in $YFeO_3$ platelets of different thicknesses, cut perpendicular to the optic axis. The thicknesses are: a) 750 μm, b) 515 μm, and c) 210 μm.[38]

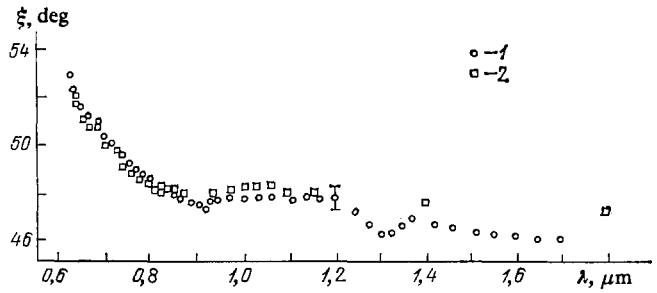

FIG. 4. Angle between the optic axis and the [001] axis in the (100) plane for: 1) $YFeO_3$ and 2) $DyFeO_3$.[44,45]

lengths 0.63 and 1.15 μm they are inclined at angles 52 and 47° to the [001] axis.[39,43–45] As a result, in these crystals the small ferromagnetic moment possesses a nonzero component along the direction of the optic axes. Figure 4 shows the wavelength dependence of the angle ξ between the optic axis and the [001] axis for $YFeO_3$ and $DyFeO_3$ in the 0.62–1.8 μm wavelength region.[44,45] The dispersion dependences of the Faraday effect in the indicated orthoferrites are shown in Fig. 5.[44,45] At the wavelength 0.63 μm the specific rotations of the polarization plane in them are respectively equal to -2900 deg/cm and -3900 deg/cm. This ensures a very high optical contrast between the domain structures in platelets cut perpendicular to the optic axis. A stripe domain structure occurs in a platelet cut in such a way that the small ferromagnetic moment lies in a plane perpendicular or inclined to the sample plane. Kurtzig and Shockley[46] have observed stripe domain structures in $YFeO_3$ and $ErFeO_3$ platelets cut in the above-indicated manner. But they did not determine the direction of the optic axis, and the contrast between the observed domain structures was, in accordance with (1.11), low. Highly-contrasting strictly periodic stripe domain structures have been observed in orthoferrite platelets cut perpendicular to the optic axis.[47,48] The DW in such platelets are strictly straight and perpendicular to the [100] axis lying in the platelet plane. They are walls of a type intermediate between the Bloch and Néel types, since the magnetic moment in them rotates in the (010) plane. Below we shall call them intermediate-type walls. Figure 6 shows a photograph of the stripe structure in a $TmFeO_3$ platelet at 137 °K. The difference between the angles of rotation of the polarization plane for oppositely magnetized domains is close to 60°. The intensities of the light beams that get transmitted through neighboring domains differ by a factor of several hundred. The stripe domain structure constitutes for light a phase diffraction grating. A theory of light diffraction by such gratings is constructed in Refs. 49 and 50. Figure 7 shows a photograph of the diffraction pattern for laser light diffracted by the stripe domain structure in a $TmFeO_3$ platelet.[47,48] The experiment was performed in zero magnetic field, and the sample temperature—100 °K—was chosen in the vicinity of the reorientation region, where the domain dimensions are small. The even diffraction orders are, in accordance with the theoretical results obtained in Refs. 49 and 50, absent in the absence of an external magnetic field. The fact that the high diffraction orders are clearly visible indicates a very high degree of periodicity of the stripe structure and a high degree of homogeneity of the orthoferrite platelets.

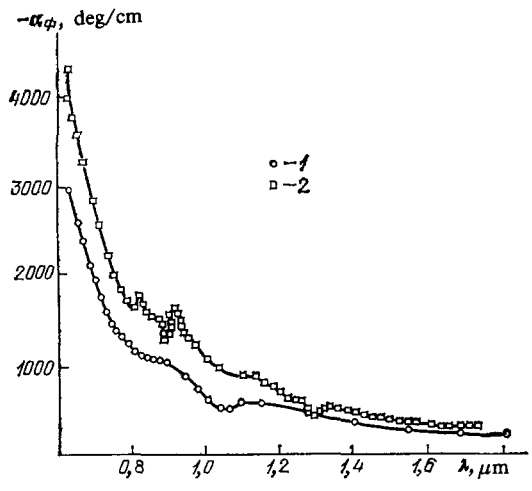

FIG. 5. Specific Faraday rotation in $YFeO_3$ (1) and $DyFeO_3$ (2).[44,45]

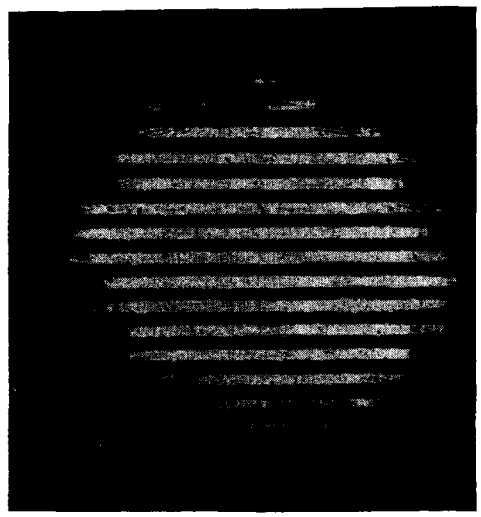

FIG. 6. Stripe structure in a $TmFeO_3$ platelet cut perpendicular to the optic axis at $T = 137$ °K (12×).[47,48]

2. EXPERIMENTAL STUDY OF DOMAIN-WALL DYNAMICS

a) Methods

The first method for the investigation of DW dynamics in ferromagnets was developed by Sixtus and Tonks.[9] The essence of the method consists in the measurement of the time of travel by a DW of a given distance along a long, thin sample of the material under investigation.

Initially, this method was used to investigate the DW velocity in Fe–Ni wires. It is precisely in Ref. 9 that the concept of a DW as the boundary layer between two oppositely magnetized domains was first introduced.

The DW transit time was measured with the aid of a ballistic galvanometer in the circuit of one of the lamps of a

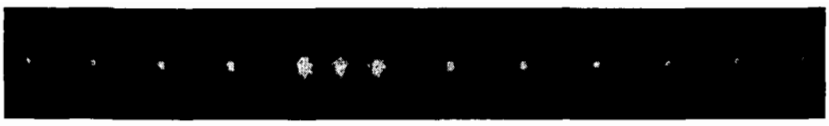

FIG. 7. Light diffraction by the stripe structure in $TmFeO_3$.[47,48]

single-shot multivibrator. The current through this lamp started at the moment when the DW crossed the first coil and stopped at the moment when the wall crossed the second coil. It was found that the dependence $v(H)$ is linear in the region of velocities up to 250 m/sec. Tsang and his collaborators[51–53] used this method to investigate DW dynamics in the orthoferrites. The orthoferrite sample had the shape of a rod of 2×2-mm square cross section and length 50 mm. There was produced at one end of the rod with the aid of a local coil a domain magnetized in the direction opposite to the direction of magnetization of the remaining part of the rod, and separated from this part by a single DW (Fig. 8). At zero time a current pulse was fed to the coil inside which the sample under investigation had been mounted. This disturbed the equilibrium of the domains, and the DW was set in motion along the rod. On crossing the boundaries of two minature coils,the DW generated in the coils voltage pulses that could be recorded on the screen of an oscillograph. By dividing the distance between the coils by the timelag between the two pulses, the sought velocity value could easily be found. It should be emphasized that many modern methods of investigating DW dynamics are modifications of the Sixtus-Tonks technique.

For the determination of the DW velocity Bobek[54] proposed a bubble collapse method (see also Refs. 11, 12, and 55). In this method the length of the magnetic-field pulse during which the radius of a bubble decreases to its critical value—the collapse radius, or the value at which the bubble loses its radial stability and disappears—is measured. The bubble radius before the application of the pulsed magnetic field and the collapse radius in the static regime are measured with the aid of the Faraday effect in a polarizing microscope. The collapse radius in the dynamical regime is difficult to determine, and, to find it, we have to use theoretical computations,[56] or more modern experimental techniques. Thus, Humphrey's high-speed photography method[57] has shown that the bubble diameter just before the disappearance in the dynamical regime is significantly smaller than the corresponding diameter in the static regime. The belief is expressed in Ref. 58, which reports the investigation of DW dynamics in yttrium orthoferrite by the bubble collapse method, that the collapse radius in the dynamical regime is two times smaller than the radius in the static regime. In Ref. 59 this difference is taken, in accordance with Ref. 56, to be smaller. Furthermore, bubbles in orthoferrite platelets have an elliptical shape, which arises as a result of the presence of anisotropy in the basal plane. Therefore, in Refs. 58 and 59 the mean of the semiaxes of the ellipse is taken as the initial bubble radius. For the above-noted reasons, the accuracy of the bubble collapse technique, as applied to the orthoferrites, is not too high.

Significantly more accurate for the investigation of DW dynamics in the orthoferrites were the magneto-optical methods of measuring the time required by a DW to cover a given distance. This procedure, with the use of the Kerr effect, was first applied to metallic ferromagnetic films.[60] In the experiments reported in Refs. 61–64, a magneto-optical method of measuring the time required by the wall to cover a given distance was used to investigate DW dynamics in the orthoferrites. It is a magneto-optical analog of the Sixtus-Tonks method, and can be applied to any transparent magnetic material in which the rotation of the polarization plane is considerable. The schematic outline of the method is explained in Fig. 9. A ray from a He–Ne cw laser was split with the aid of a birefringent $CaCO_3$ platelet into two rays polarized in mutually perpendicular planes. Both rays were focused on the surface of an orthoferrite platelet cut perpendicular to either the optic axis,[61–63] or the [001] axis.[64] A two-domain structure with a single DW was obtained in the platelet under investigation with the aid of a gradient magnetic field perpendicular to the sample surface. For orthoferrite platelets cut perpendicular to the optic axis, and possessing an initial stripe domain structure (see Fig. 6), a solitary intermediate-type DW oriented perpendicularly to the axis and surface of the plate was obtained in a magnetic field with a gradient of 300 Oe/cm (Fig. 10). In plates cut perpendicu-

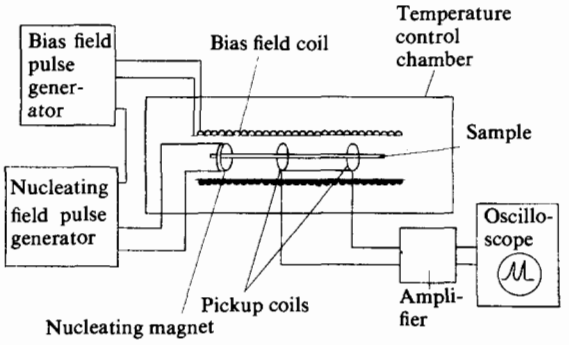

FIG. 8. Diagrammatic representation of the Sixtus-Tonks procedure for measuring the domain-wall velocities in orthoferrites.[53]

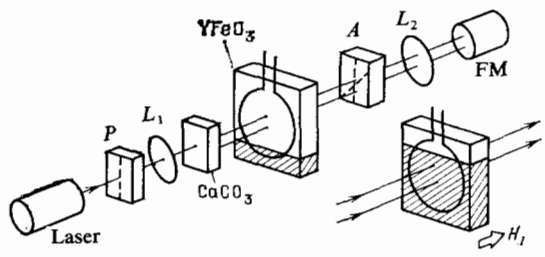

FIG. 9. Experimental arrangement for the measurement of the domain-wall velocities in orthoferrites by means of the magneto-optical method of measuring the transit time over a given distance.[61b] P) Polarizer, A) Analyzer, L_1 and L_2) lenses.

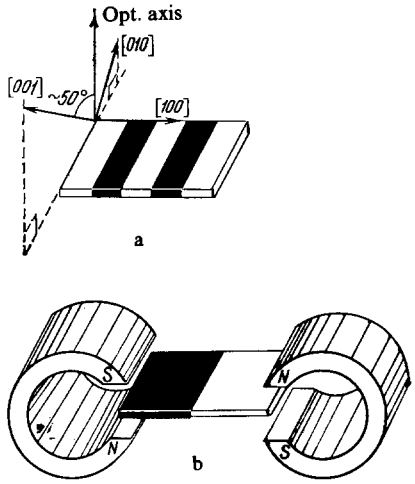

FIG. 10. a) Stripe structure[4] and b) scheme for obtaining a solitary domain wall in an orthoferrite platelet cut perpendicular to the optical axis.[61b]

lar to the [001] axis, it was possible to obtain with the aid of a magnetic field with a gradient of $(1-2)\times 10^3$ Oe/cm a two-domain configuration with a single Bloch or Néel wall.[82] The observed DW width was of the order of [62] 1μm, which is significantly greater than its computed value. Perhaps this is due to the inclination of the DW to the sample surface and to diffraction effects. The two pulses corresponding to the instants when the moving DW passed through two light spots were recorded with the aid of a photomultiplier on the screen of a stroboscopic oscillograph or on the tape of a recorder. Knowledge of the distance between the light spots on the sample and the determination of the time lag between the two indicated pulses made it possible to find the velocity of the stationary DW motion. Rectangular orthoferrite platelets with thickness about 100 μm and transverse dimensions 3×3 mm^2 were used. Coils of diameter 0.5–2 mm that produced pulsed magnetic fields of intensity up to 5 kOe were glued to the highly chemically polished facets of the platelet at points far from its edges (either directly, or through a thin glass). This made it possible to substantially increase the region of operating magnetic fields for the investigation of DW dynamics in comparison with the fields used in the Sixtus-Tonks method.[53] In the latter method the region of investigations was limited to pulsed fields of intensity ~ 160 Oe, since new domains began to appear at the edges of the orthoferrite bar in stronger fields, and this led to an ambiguity in the determination of the DW velocity.

Much more universal is the high-speed photography method, which is also based on the Faraday effect, and is suitable for transparent magnetic materials. This method allows us to record the dynamic domain structure on a photographic film or on the magnetic tape of a video recorder. The single exposure of the ferromagnetic sample with domain structure is accomplished with short light pulses from different types of lasers: a neodymium-containing-yttrium–aluminum-garnet laser,[65] dye lasers pumped by a pulsed nitrogen laser,[66] as well as mode-locked gaseous lasers.[67] For the investigation of DW in ferromagnets, light pulses of duration about 10 nsec were usually employed. This duration was quite adequate for the investigation of DW and bubble dynamics in ferrite-garnet films, in which the DW and bubble velocities do not exceed a few score, or, in specific cases, a few hundred meters per second. If the DW motion is stationary, then we can, by varying the time lag between the commencement of the magnetic-field pulse and the light pulse, obtain a sequence of photographs of the dynamic domain structure, and determine the DW velocity from it. Since the Faraday effect in ferrite-garnet films is not strong, we must use an image intensifier to increase the contrast of the dynamic domain structure.[67–69] In a number of cases the dynamics of the DW of bubbles in ferrite-garnet films was investigated by the time scanning the bubble image.[69,70]

If the light was insufficient for an image of the dynamic domain structure to be obtained in a single exposure, then the stroboscopic technique was used in the case of stationary DW motion. This technique has, in particular, been used to determine the DW mobility in the orthoferrites,[71] and to determine the DW velocity in orthoferrite platelets cut perpendicular to the [001] axis.[72] In this investigation, a single photograph of the dynamic domain structure required an exposure ranging from several score minutes to hours. This long exposure was necessary for two reasons. First, the power of the semiconductor laser used was low; secondly, the influence, described in Sec. 1c, of the crystal birefringence on the Faraday effect is strong, with the result that the angle of rotation of the major axis of he resulting ellipse at the exit from a platelet of the indicated orientation does not exceed 1–2°. The above-described procedure for measuring the DW's transit time between two fixed light spots is also a stroboscopic procedure.

Shorter light pulses are required for the high-speed photography of the DW dynamics in the orthoferrites, in which the DW velocity is significantly higher than in the ferrite-garnets. So far such investigations have been carried out with the use of light pulses of duration 10 nsec,[73] 6 nsec,[74,75] and 1 nsec.[76,77]

In these experiments DW dynamics was investigated in yttrium orthoferrite platelets cut perpendicular to the optic axis, where the Faraday effect is proportional to the thickness, and is equal to 2900 deg/cm at a wavelength of 0.63 μm. This ensures a very high optical contrast of the dynamic domain structure, and makes it possible to obtain a photograph of this structure in a single exposure of the sample under investigation. In the experiments reported in Refs. 76 and 77, 1-nsec light pulses from an oxazine-dye laser pumped by a nitrogen laser with transverse discharge[78] were used. The red dye-laser light beam was split into two with the aid of mirrors (Fig. 11).[77] With the aid of additional mirrors there was introduced into the second beam a controlled delay, the length of which could be varied from 3 to 30 nsec by varying the distance between the additional mirrors. Each light beam passed through a separate polarizer, and was then focused on the sample under study. By properly choosing the polarization directions in the two beams, it was possible to ensure opposite contrasts for the dynamic domain structures obtained with the aid of each of the two beams. This in turn made it possible to get two dynamic domain structures on

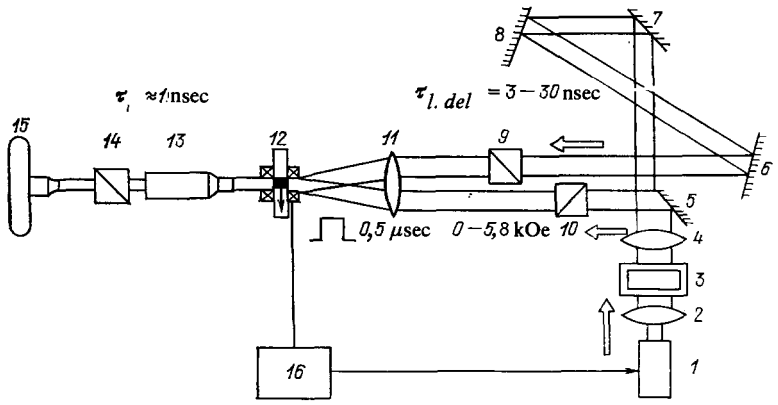

FIG. 11. Diagram of experimental arrangement for double-shot high-speed photography of domain wall dynamics. 1) laser; 2), 4), and 11) lenses; 3) cell with dye; 5)–8) mirrors; 9), 10), and 14) polarizers; 12) orthoferrite platelet; 13) microscope; 15) camera; 16) assembly of pulse generators.[77]

the same photograph with a single dye-laser light pulse in the course of one passage of the DW through the sample. The sample region traversed by the DW during the time lag between the two light pulses could be recorded in the form of a very high-contrast dark or bright stripe directly on a photographic plate of high sensitivity without the use of an image intensifier. Figure 12 shows an example of the photographs obtained in this manner of the two positions of the dynamic domain structure in yttrium orthoferrite.

A typical $v(H)$ curve, obtained over a broad range of magnetic fields by the above-indicated methods, is shown in Fig. 13. The following characteristics are noteworthy: the presence of a linear section $v = \mu H$ in the region of weak fields, sharp anomalies of the type of "small shelves" at selected values of the velocity, and "saturation" of the velocity in strong fields. Let us discuss these characteristics in turn.

b) DW Mobility

On the linear segmentof the $v(H)$ curve a characteristic of the dynamical properties of the DW is the mobility μ, defined by the formula

$$\mu = \lim_{H \to 0} \frac{v(H)}{H}. \qquad (2.1)$$

Virtually all the above-described methods are used to investigate the DW mobility in the orthoferrites. In Rossol's experiments reported in Refs. 71 and 79 the stroboscopic technique based on the utilization of the Faraday effect was used to investigate the DW mobility in the orthoferrites. The frequency dependence of the amplitude of the DW displacement from the equilibrium position under the action of a field with frequency as high as 10^7 Hz was determined experimentally. It was shown that this dependence has a relaxational character, i.e., that in the range of frequencies used the DW inertia is insignificant. The DW mobilities in the orthoferrites $YFeO_3$, $TmFeO_3$, $EuFeO_3$, $LuFeO_3$, $HoFeO_3$, and $ErFeO_3$ were determined over a broad range of temperatures from the relaxation frequencies. It is shown in Ref. 79 that the DW mobility in $YFeO_3$ is strongly temperature dependent, and varies from 6×10^3 cm/sec-Oe at 300 °K to 5×10^4 cm/sec-Oe at 77 °K (Fig. 14). We must draw attention to the record-high DW mobility in $YFeO_3$ at 77 °K. The DW mobility in the orthoferrites has not been directly investigated at lower temperatures. Indirect data on it can be obtained from nuclear magnetic resonance data.[80]

We note the following important circumstance. The above-indicated results were obtained in a $YFeO_3$ sample that was prepared with particular care, so as to reduce to a minimum the effect of the surface roughness and the impurities in the crystal on the DW mobility. The final mechanical polishing of the sample was combined with chemical polishing. The coercive force in the sample obtained in this manner, called in Rossol's paper sample A, was equal to 0.1 Oe. In another sample (sample B), obtained by the same meth-

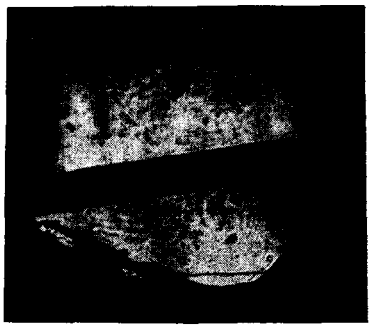

FIG. 12. Photograph of two dynamic domain structures in $YFeO_3$, taken during one passage of the domain wall through the sample. The darkened band is the portion of the sample traversed by the domain wall during the time interval between two light pulses.

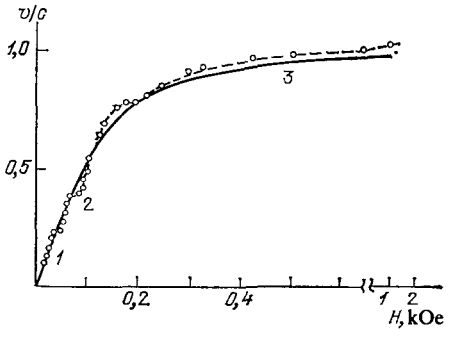

FIG. 13. Typical magnetic-field dependence of the ratio of the domain-wall velocity to the limiting velocity. 1)–3) the most characteristic parts of the $v(H)/c$ curve: 1) linear-dynamics region; 2) region of the magnetoelastic anomalies; 3) velocity saturation region. The continuous curve depicts the theoretical dependence.

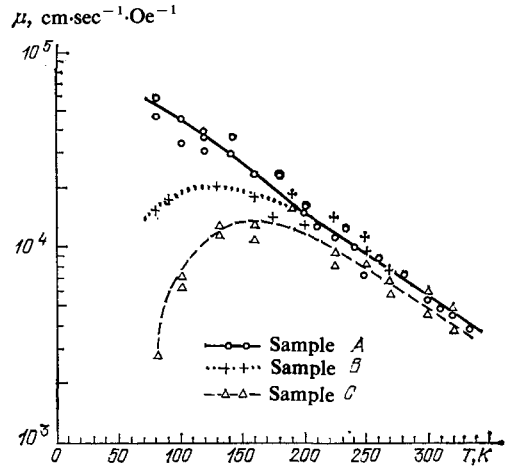

FIG. 14. Domain-wall mobility in $YFeO_3$ as a function of the temperature.[79]

od, the mobility increased as the temperature was lowered to 110 °K, and then began to decrease slowly. In a sample, *C*, that was subjected to a rougher mechanical polishing followed by annealing the mobility began to fall sharply at as high a temperature as 140 °K. Thus, the value of the DW mobility and, especially, its temperature dependence are essentially determined by the quality of the sample. The causes of the decrease of the mobility in samples *B* and *C* are not entirely clear. Most probably, this is due to the presence in the orthoferrite lattice of Fe^{4+}, Fe^{2+}, and rare-earth ions, or to crystal defects. The higher-quality sample *A* should be expected to exhibit DW-relaxation characteristics governed by internal processes (interaction with the thermal quasiparticles), whereas in the samples *B* and *C* the interaction with the defects and impurities was the dominant process.

Huang,[81] apparently, was the first to point out that the DW mobility in the sample *A* of $YFeO_3$ used in Rossol's experiment[79] varied with temperature like $1/T^2$, and was the first to relate this fact to a four-magnon relaxation process. In his analysis he considered the orthoferrite to be a ferromagnet, ignoring its sublattice structure. The good agreement obtained in Ref. 81 between the experimental and calculated DW mobilities in $YFeO_3$ for the sample *A* used in Rossol's experiment is accidental. We present the current theoretical ideas about DW mobility in the orthoferrites below (see Sec. 3c).

The DW-mobility anisotropy in yttrium orthoferrite has been investigated by Shumate,[82] as well as by Tsang, R. L. White, and R. M. White.[51-53] For this purpose, the last authors used the Sixtus-Tonks method. Figure 15, which was taken from Ref. 53, shows the magnetic-field dependences of the velocities of the Bloch, Néel, and head-to-head DW at room temperature. In Ref. 52 the Bloch- and Néel-DW mobilities in the temperature range from 250 to 600 °K are determined from the initial sections of the $v(H)$ curves. These data supplement and agree with Rossol's earlier data.[79] At room temperature $\mu_B = 6.16\times10^3$ cm/sec-Oe and $\mu_N = 5.8\times10^3$ cm/sec-Oe. They are slightly higher than the values obtained by Shumate,[82] but the ratio $\mu_B/\mu_N = 1.06$ is the same and agrees with the theoretical calculations based on a phenomenological consideration of the relaxation (Rosencwaig,[83] Gyorgy and Hagedorn[84]).

c) Magnetoelastic anomalies

As the magnetic field intensity is increased, the DW dynamics in the orthoferrites becomes essentially nonlinear. It can be seen from Fig. 15 that there are quite broad regions of constancy of the DW velocity (small shelves) on the linear $v(H)$ curves for all the DW's in $YFeO_3$ that were investigated in the experiments reported in Ref. 53. In the case of the Néel DW such a shelf occurs at a velocity of 4 km/sec. On the $v(H)$ curve for the Bloch DW the anomalies can be seen clearly at velocities of 4 and 8 km/sec. As H increases further, the Bloch- and Néel-DW velocities rise to 13 km/sec without any visible saturation.

Similar nonlinearities on the $v(H)$ curves for the DW in the orthoferrites have been observed also by the bubble-collapse method,[59] by the method of measuring the transit time of a DW over a given distance,[61] and by the methods of single-shot[74] and double-shot[76,77] high-speed photography. Figure 16 shows the magnetic-field dependence, obtained by the bubble-collapse method,[59] of the DW velocity in a $YFeO_3$ platelet cut perpendicular to the [001] axis. The bias fields H_b were equal to 22.3 and 23.7 Oe. The $v(H)$ curve exhibits a very weak anomaly at a velocity of 4.8 km/sec, according to Ref. 59, and more distinct ones at velocites of 7 and 14 km/sec. No DW-velocity saturation was observed in magnetic fields of intensity up to 370 Oe, and the maximum DW velocity was 25 km/sec. Attempts to relate the $v(H)$ anomalies in yttrium orthoferrite at the velocities 4 and 7 km/sec with the Walker velocity limit by taking account of the orthorhombic magnetic anisotropy of the crystal turned out to be unsound.[85] It is shown in Refs. 51 and 52 that the above-indicated DW-velocity values correspond to the longitudinal- and transverse-sound velocities in yttirum orthoferrite. It should be emphasized that the weakly ferromagnetic ortho-ferrites became the first magnetically ordered materials in which the DW velocity reached and exceeded the velocity of sound.

Tsang and White's interpretations[51] of the $v(H)$ singu-

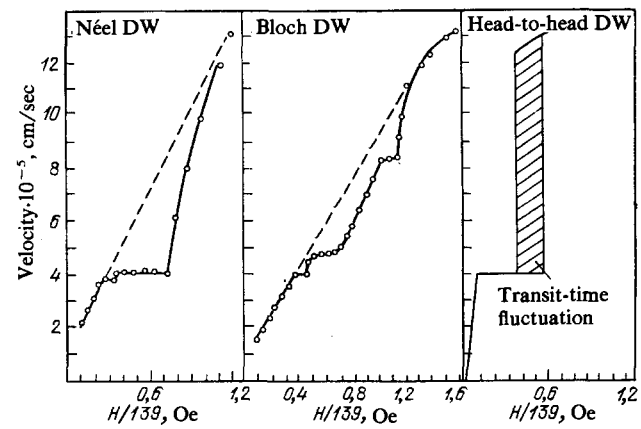

FIG. 15. Curves of velocity as a function of magnetic field obtained for different types of domain wall in $YFeO_3$ by the Sixtus-Tonks method.[53]

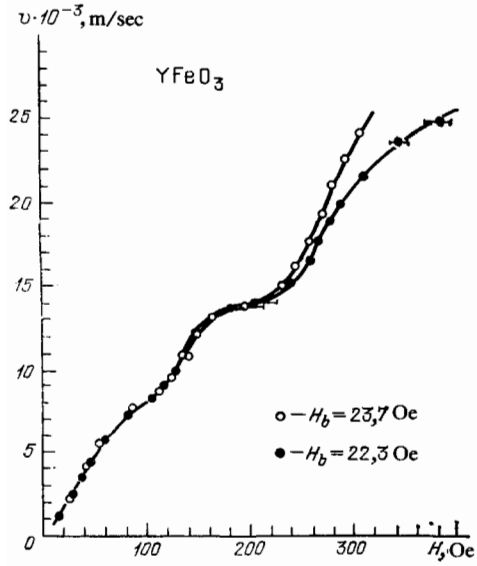

FIG. 16. Curve of $YFeO_3$ domain wall velocity as a function of magnetic field obtained by the bubble-collapse method.[59]

larities at the velocities 4.3 and 7 km/sec in $YFeO_3$ are corroborated by the experimental data obtained for $TmFeO_3$ in the investigations reported in Refs. 61 and 64. These investigations, in which the dynamics of intermediate type DW was studied, revealed similar $v(H)$ anomalies at $v = 3.3$ and 6.2 km/sec, which are close to the velocities of transverse and longitudinal sound in this orthoferrite.[86] In $YFeO_3$ samples of thicknesses ranging from 100 μm to 2 mm the indicated regions have widths of several tens of oersteds for all the types of DW investigated. Significantly broader regions of constancy of the velocity are observed in thinner samples.[76] For Bloch DW in a $YFeO_3$ sample of thickness 25 μm, cut perpendicular to the [001] axis, the region ΔH_t is scarcely noticeable, while ΔH_l is equal to 500 Oe. For the Néel DW, $\Delta H_t = 250$ Oe, i.e, $\Delta H_t \sim \Delta H_l$ (see Fig. 22 below). As we shall show below in Sec. 4, these anomalies are due to the Cherenkov emission of phonons during the motion of the DW. This emission is most intense when the DW velocity is close to s_t or s_l, where $s_{l,t}$ are the longitudinal: and transverse-sound velocities. The theory gives estimates for the widths of the intervals ΔH_t and ΔH_l. In particular, it can be shown that, for the Bloch DW, $\Delta H_t \ll \Delta H_l$. This is confirmed by the above-described experiment.[76] Let us note that, on the whole, there is good qualitative agreement between the experimental and theoretical data on the magnetoelastic anomalies in the orthoferrites. Additional investigations are required for comparison to be possible. In particular, the expressions contain the sound attentuation constant η, which has been experimentally determined only for $ErFeO_3$.[87] This makes a quantitative comparison of the theory with experiment difficult.

d) Limiting velocity

The method of measuring the transit time of a DW over a given distance between two light spots turned out to be a significantly more accurate method for the investigation of the DW velocity in WFM than the bubble-collapse and Sixtus-Tonks methods. References 61–64 report investigations of the velocity of intermediate-type DW in orthoferrite platelets cut perpendicular to the optic axis. Figure 17, which was taken from Ref. 62, shows the magnetic-field dependence of the DW velocity in $YFeO_3$ at 300 °K. In magnetic fields of from 20 to 300 Oe the $v(H)$ curve is in accord with the results obtained in earlier investigations, and shown in Figs. 15 and 16. But a comparison of these figures with Fig. 17 reveals an appreciable difference. The DW velocity attains a value of 20 km/sec in a magnetic field of intensity 600 Oe, and subsequently remains constant as the magnetic field intensity is raised to 1000 Oe. The indicated velocity has the meaning of a limiting DW velocity in the orthoferrite. Thus, the technique employed in the investigations reported in Refs. 61 and 62 made it possible for the first time to find the limiting DW velocity in an orthoferrite experimentally.

It is shown in Refs. 62 and 88 on the basis of an analysis of the asymptotic behavior of the magnetization in the DW that the limiting DW velocity in the orthoferrite coincides with c, the phase velocity of the spin waves on the linear section of the spectrum. This velocity, in the leading approximation, depends only on the exchange constants of the ortho-ferrite. In terms of the constants α and β introduced above [see the formula (1.6)], the velocity c is given by the formula

$$c = \frac{1}{2} gM_0 \sqrt{\alpha\delta}. \tag{2.2}$$

It is convenient to rewrite it in terms of the gap ω_1 in the lower-magnon-branch spectrum and the DW thickness x_0: $c = \omega_1 x_0$ (Ref. 62). For an order-of-magnitude estimate of c, we can use the formula $c \sim akT_N/\hbar$.

To the linear section of the spectrum corresponds a broad range of wave-vector values: $x_0^{-1} \ll k \ll a^{-1}$ (see Fig. 18, which was taken from Ref. 53b, and Sec. 3).

The value of c determined from the known magnon spectrum (see Fig. 18), as well as the value computed from the formula (2.2), is in good agreement with the experimental value for the limiting DW velocity. Indeed, setting

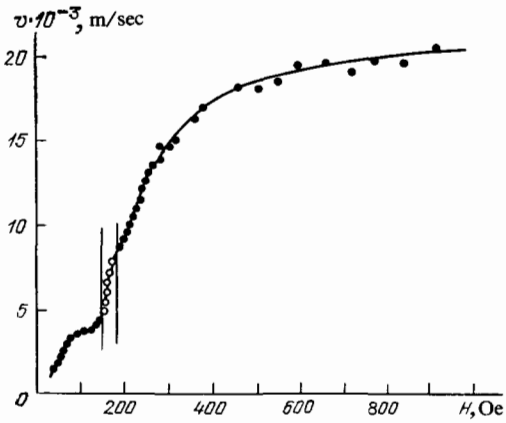

FIG. 17. Magnetic field dependence of the velocity of the intermediate type domain wall in $YFeO_3$, obtained by the method involving the measurement of the DW transit time over a given distance between two light spots.[62]

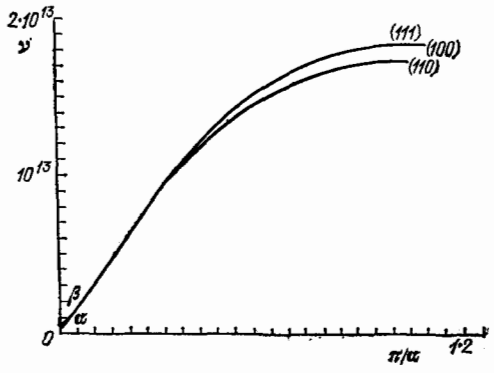

FIG. 18. Magnon spectrum in $YFeO_3$, computed from the known values of the exchange integrals within the boundaries of the Brillouin zone.[53b]

$g = 1.76\times 10^7$ (Oe-sec)$^{-1}$, $H_E = \delta M_0/2 = 6.4\times 10^6$ Oe, and $A = \alpha M_0^2/2 = 4.4\times 10^{-7}$ Oe/cm, we obtain for c the value 2×10^6 cm/sec, which is in good agreement with experiment.

Let us note two important circumstances. First, the spin-wave velocity in the orthoferrites depends quite weakly on the direction of propagation (see Fig. 18). Experimental analysis[64,75] has demonstrated that the limiting DW-velocity values are quite truly isotropic: the Bloch- and Néel-DW velocities have virtually the same values in $YFeO_3$. Secondly, the expression for the limiting DW velocity contains only the exchange constants α and δ, and does not (in contrast to the expression for the Walker limiting DW velocity in ferromagnets) contain the anisotropy constants. The values of the exchange constants for the various orthoferrites are close; consequently, the values of the limiting velocities should also be close. Furthermore, the exchange constants of the orthoferrites vary slowly as the temperature is lowered from room temperature to liquid-nitrogen temperatures. The limiting velocity of the intermediate-type DW has the same value in $TmFeO_3$ at °K as in $YFeO_3$ at room and liquid-nitrogen temperatures.

All these facts, added to the equality of the numerical values of the magnon phase velocity and the limiting DW velocity, confirm the correctness of the theoretical concept of a limiting DW velocity in the WFM.

A rigorous theoretical demonstration of the existence of a limiting DW velocity in the orthoferrites and a theory of forced DW motion are given in Refs. 89–91, and are described in Sec. 3 of the present review.

e) DW dynamics in iron borate

Nonlinear DW dynamics was for a long time investigated mainly in orthoferrites. It is of interest to study the dynamical properties of DW in other weak ferromagnets differing in magnetic structure, symmetry, or the type of magnetic anisotropy from the orthoferrites.

A promising object for such investigations is iron borate $FeBO_3$ an easy-plane weak ferromagnet with space symmetry group D_{3d}^6. The existing techniques allow us to obtain high-grade $FeBO_3$ single crystals that are transparent in the optical region, and to produce and investigate solitary DW's in these crystals.

Kim and Khvan[92] have investigated DW dynamics in $FeBO_3$ by the method of forced nonlinear oscillations. The $v(H)$ curve they obtained in these investigations exhibits anomalies at velocities of 0.5 and 3.6 km/sec, with subsequent growth of the velocity. Anomalies at the sound velocities and a limiting velocity were not observed.

Recently, DW dynamics in $FeBO_3$ single crystals was investigated by the stroboscopic technique.[93] Figure 19 shows the $v(H)$ curve at 290 °K. As can be seen from the figure, the DW mobility is equal to 5×10^4 cm/sec-Oe, which is significantly higher than the mobility at the same temperature in $YFeO_3$. Also clearly visible on this same figure are regions of constancy of the DW velocity at 4.6, 7.0, and 10.5 km/sec, which correspond to the two transverse- and longitudinal-sound velocities.[94] The widths of the shelves are small (of the order of 3 Oe), and, perhaps, this is why they were not observed in the experiment reported in Ref. 93. A limiting DW velocity, equal to 14.2 km/sec, has, for the first time, been observed in $FeBO_3$. The value of the limiting DW velocity corresponds to the velocity of the spin waves on the linear section of their dispersion law.[94]

According to theory,[88,31] the limiting DW velocity in all antiferromagnets and weak ferromagnets with an even principal axis[5)] is equal to the value of c.

According to experiment,[93] the principal properties of moving DW are the same for essentially different WFM: the rhombic orthoferrites with strong anisotropy in the basal plane and the easy-plane $FeBO_3$. This is consistent with current theory, and allows us to conclude that the laws of nonlinear DW dynamics are the same in all the WFM.

It must be noted that the limiting velocities in the WFM (20 km/sec in the orthoferrites and 14.2 km/sec in iron borate) are the maximum DW velocities that have been attained to date in magnetically ordered materials. Limiting velocities of this order of magnitude should be realized in other WFM with a high Néel temperature. The very good agreement between the experimental value for the limiting DW velocity and the theoretical result indicates the adequacy of the proposed mathematical description of the DW dynamics in the WFM.[88–91] The reason for this adequacy lies in the stability of the dynamic DW structure in the WFM right

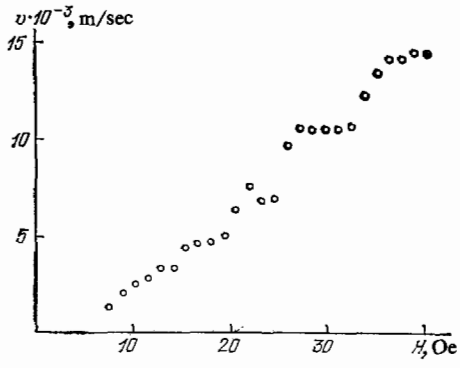

FIG. 19. Magnetic field dependence of the velocity of a 180° domain wall in $FeBO_3$.[93]

up to the limiting velocities.

In the case of the ferrite-garnets, to account for the saturation velocities, which are of the order of a few score meters per second, we must use an empirical relation.[12] The deviation of the limiting DW velocites in epitaxial ferrite-garnet films from the Walker limiting velocity is caused, as we have already noted, by a substantial complication of the structure of the moving DW. Physically, this is due to the fact that a substantial reconstruction of the DW structure occurs in ferromagnets in fields of the order of the anisotropy field H_A, which, in these materials is comparable to the demagnetizing field. The situation is different in the WFM: the rotation of the magnetization vector occurs in magnetic fields of the order of $\sqrt{H_E H_A}$,[16,17,25] i.e., in fields significantly stronger than the magnetostatic fields. This fact, together with the high DW mobilities in the WFM, greatly broadens the range of pulsed magnetic fields in which experimental investigations of nonlinear DW dynamics can be carried out.

3. THEORY OF DOMAIN WALL MOTION IN WEAK FERROMAGNETS

Let us consider the dynamics of the magnetization of a WFM in the two-sublattice model. The dynamics of a magnetic material is described on the basis of the system of Landau-Lifshitz equations[4] for $\mathbf{M}_1$ and $\mathbf{M}_2$. As shown in the papers of Ref. 31, this system can, under the natural assumption that $|\mathbf{m}| \ll |\mathbf{l}|$, be reduced to a single equation for the unit (normalized) antiferromagnetism vector $\mathbf{l}$.

a) Effective equations

The dynamical equation for the vector $\mathbf{l}$ allows a unified description of both spin waves in AFM and the essentially nonlinear processes, in particular, the DW motion. Let us note that the equation for the vector $\mathbf{l}$ has been analyzed in detail in connection with the general problem of the low-frequency dynamics of the multisublattice AFM with a noncoplanar orientation of the magnetic moments.[95]

In the absence of an external magnetic field the equation of motion for the vector $\mathbf{l}$ has the form[31,95]

$$\left[\mathbf{l},\ \left(c^2\Delta\mathbf{l} - \frac{\partial^2\mathbf{l}}{\partial t^2} - \chi_\perp^{-1}(gM_0)^2\frac{\partial w_a}{\partial \mathbf{l}}\right)\right] = 0, \qquad (3.1)$$

where $\chi_\perp = 4/\delta$ is the transverse—with respect to the equilibrium orientation of the vector $\mathbf{l}$—component of the magnetic susceptibility, w_a is the effective magnetic-anisotropy energy, and c is given by the formula (2.2).

The large factor $1/\chi_\perp$ in front of the anisotropy energy in the formula (3.1) describes the exchange enhancement of the magnetic anisotropy of the AFM or WFM.

The magnetization of the WFM is given by the formula

$$m = \frac{1}{\delta}[\mathbf{dl}] + \frac{2}{\delta}(\mathbf{h} - \mathbf{l}(\mathbf{hl})) + \frac{2}{g\delta M_0}\left[\frac{\partial \mathbf{l}}{\partial t},\ \mathbf{l}\right]. \qquad (3.2)$$

The first two terms in this formula occur in the static case as well [see formula (1.5)]. The last term is due to the appearance of additional noncollinearity of the sublattice magnetizations, which arises as a result of their precession. This term makes the magnetization dynamics in a ferromagnet essentially different from the magnetization dynamics in a WFM.

Let us note that the equation of motion (3.1) with $h \neq 0$ is "Lorentz-invariant" in the sense that the time and space derivatives enter into it in the form of the combination $c^2\Delta$, $\partial^2/\partial t^2$. This enables us to obtain the solution corresponding to a uniformly moving DW from the known solution for the stationary DW through a simple Lorentz transformation.

A number of effects of DW dynamics are determined by the interaction of the DW with the elementary excitations of the magnetic material, first and foremost with the spin waves (the magnons). It is not difficult to verify that Eq. (3.1) describes two spin-wave branches. To do this, we must consider that ground state in which the vector $\mathbf{l}$ is oriented along the a axis. As follows from the linearized equation (3.1), to small oscillations of $\mathbf{l}$ about this state correspond waves polarized along the b and c axes, and obeying the dispersion law[16,17,96]

$$\omega_1^2(k) = \omega_1^2 + c^2k^2, \qquad \omega_2^2(k) = \omega_2^2 + c^2k^2, \qquad (3.3)$$

where k is the wave vector, and the quantities

$$\omega_1 = \frac{1}{2}gM_0\sqrt{\delta\beta_1}, \quad \omega_2 = \frac{1}{2}gM_0\sqrt{\delta\beta_2} \qquad (3.4)$$

have the meaning of magnon activation. Physically, the quantity c has, as can easily be seen from (3.3), the meaning of the phase velocity of the spin waves on the linear section of the spectrum. It is also easy to verify that c is equal to the minimum phase velocity of the waves with the dispersion law (3.3).

The formulas (3.3), like the Eq. (3.1), were derived in the long-wave approximation, and are valid only when $\lambda \gg a$, where λ is the characteristic inhomogeneity dimension. Since $\sqrt{\alpha/\beta} = x_0 \gg a$, the spectrum (3.3) can be used in the broad wave-vector range $k \ll 1/a$. For $k \gg 1/x_0, \omega_{1,2} = ck$

The band character of the magnon spectrum begins to manifest itself when $k \sim 1/a$, and the long-wave approximation cannot be used in this region (see Fig. 18 in Chap. 2).

The activation frequencies ω_1 and ω_2 have been measured for a number of antiferromagnets and WFM with the use of antiferromagnetic resonance[98] and with the aid of light scattering.[99] For the orthoferrites ω_1 and ω_2 are usually close to 11–13 cm^{-1} and 15–20 cm^{-1}, respectively (let us recall that 1 cm^{-1} corresponds to 30 GHz).

There arise in the presence of DW in WFM two additional magnon branches localized near the DW [surface magnons (SM)]. The SM dispersion law can be written in the form[53b]

$$\omega_1(k_\perp) = c|\mathbf{k}_\perp|, \quad \omega_2(k_\perp) = \sqrt{\omega_2^2 - \omega_1^2 + c^2k_\perp^2}, \qquad (3.5)$$

where $\mathbf{k}_\perp$ is the wave vector in the plane of the DW. The surface magnons with the nonactivation dispersion law $\omega_1(\mathbf{k}_\perp)$ describe the flexural vibrations of the DW. In writing down (3.5), it is assumed that $\beta_2 > \beta_1$, i.e., that rotation in the a–c plane is energetically advantageous at the wall. To the $\omega_2(\mathbf{k}_\perp)$ wave corresponds the mutual oscillation of the $\mathbf{M}_1$ and $\mathbf{M}_2$ in the bias DW without the DW as a whole. Kraftmakher *et al.*[101] have observed microwave-field absorption due to the excitation of this magnon branch in orthoferrite samples with a domain structure. In moving DW the surface-magnon energies are, on account of the Lorentz-in-

variance, given by the formula

$$\omega_{1,2}(k_\perp, v) = \frac{\omega_{1,2}(k_\perp)}{\sqrt{1-v^2/c^2}}. \tag{3.6}$$

b) Structure of moving DW

In Sec. 1 we described the structure of static DW of different types (*ac*- and *ab*-walls, Bloch walls, Néel walls, etc.). To obtain the formulas that describe moving DW, it is sufficient to use the Lorentz transformation. The angle (θ) and magnetization (**m**) distributions in the DW can be found with the aid of the formulas (1.10) and (3.2). As a result, for a wall of the *ac*-type we obtain

$$\begin{gathered} l_x = \operatorname{th}\frac{\xi - vt}{x_{01}(v)}, \quad l_y = 0, \quad l_z = \frac{1}{\operatorname{ch}[(\xi-vt)/x_{01}(v)]}, \\ m_x = -\frac{d/\delta}{\operatorname{ch}[(\xi-vt)/x_{01}(v)]}, \quad m_y = \frac{2v/g\delta M_0 x_{01}(v)}{\operatorname{ch}[(\xi-vt)/x_{01}(v)]}, \\ m_z = \frac{d}{\delta}\operatorname{th}\frac{\xi-vt}{x_{01}(v)}, \end{gathered} \tag{3.7}$$

where

$$x_{01}(v) = x_{01}\sqrt{1-\frac{v^2}{c^2}}.$$

In the course of the motion, the magnetization in this plane, in contrast to the stationary case, leaves the plane of the DW, i.e., $m_y \propto (v/c) \neq 0$. This property is also possessed by DW in a ferromagnet, the dynamics of which is governed by the Landau-Lifshitz equation.[12,14]

In an *ab*-type DW the magnetization is, as in the $v = 0$ case, always parallel to the c axis:

$$\begin{gathered} l_x = \operatorname{th}\frac{\xi-vt}{x_{02}(v)}, \quad l_y = \frac{1}{\operatorname{ch}[(\xi-vt)/x_{02}(v)]}, \quad l_z = 0, \\ m_z = \frac{d}{\delta}\operatorname{th}\frac{\xi-vt}{x_{02}(v)} - \frac{2v}{g\delta M_0 x_{02}(v)}\frac{1}{\operatorname{ch}[(\xi-vt)/x_{02}(v)]}, \end{gathered} \tag{3.8}$$

where

$$x_{02}(v) = x_{02}\sqrt{1-\frac{v^2}{c^2}}.$$

The energy of both types of DW depends on their velocity **v** or momentum **p** in a relativistic manner[89,90]:

$$\sigma = \frac{\sigma(0)}{\sqrt{1-(v^2/c^2)}}, \quad \text{or} \quad \sigma = \sqrt{\sigma^2(0)+c^2p^2},$$

where $\sigma_i(0) = 2M_0^2\sqrt{\alpha\beta_i} = 2\alpha M_0^2/x_{0i}$ is the energy of the stationary DW per unit area of wall.[29]

It follows from the formulas obtained above that a DW in a WFM cannot move with velocity greater than c. Thus, the phase velocity of the spin waves on the linear section of the spectrum determines the limiting DW velocity (this result is obtained in Refs. 62 and 88). As the wall velocity approaches the limiting value, the wall thickness decreases like[88] $\sqrt{1-(v^2/c^2)}$. It is important to note that this result does not depend on the character of the anisotropy of the WFM.

This Lorentz contraction of the DW thickness raises the question of the applicability of the formulas (3.7) and (3.8) in the description of DW as $v \to c$. Let us recall that, in the macroscopic description, the DW thickness should be much greater than the lattice constant, i.e.,

$$x_0(v) \gg a, \quad \text{or} \quad 1-\frac{v^2}{c^2} \gg \left(\frac{a}{x_0}\right)^2 = \frac{\beta a^2}{\alpha} \sim \frac{\beta}{\delta}. \tag{3.9}$$

Thus, the long-wave approximation formulas adequately describe moving DW everywhere except in a narrow ($\sim(\beta/\delta) \sim 10^{-2}$) range of velocities in the vicinity of the limiting wall velocity c.[88] Eleonskiĭ et al.[91] have obtained solutions describing the DW motion within the framework of the equations for the vectors **m** and **l** without the approximation $|\mathbf{m}| \ll |\mathbf{l}|$ or $\alpha|\Delta\mathbf{l}| \ll \delta$.. Notice, however, that in writing down the expression (1.3) for the energy of the magnetic material we in fact used the long-wave approximation condition $|\Delta\mathbf{l}| \ll 1/a^2$. Strictly speaking the expression for the energy also contains terms of the order of $\alpha a^2(\Delta\mathbf{l})^2$, which can be dropped only in the long-wave approximation.[17] In the indicated narrow region of velocities where the DW thickness is comparable to the lattice constant, we cannot, generally speaking, describe the DW in the magnetic material within the framework of the long-wave approximation for the macroscopic magnetization density, and must proceed from an analysis of the exchange interaction of the discrete spin system of the magnetic material.[88]

c) Velocity of the forced motion

The preceding analysis was peformed for the idealized case of a magnetically ordered medium without allowance for dissipation. In this case the DW wall can move "by inertia" with any velocity lower than the limiting velocity c, and the purpose of the investigation is to compute the structure of a DW moving with a given velocity.

But of greater practical importance is the problem of the computation of the velocity in the case of the stationary motion of a DW acted upon by an "external force"—as a rule, an external magnetic field H, which removes the equivalence of the states to the right and left of the DW. If the relaxation processes in the system are sufficiently weak, then the computation of the function $v(H)$ can be carried out on the basis of the known solutions for a nondissipative medium.[27] The problem can be formulated as follows: if we know the magnetization distribution in the DW, we can compute the velocity dependence of the dynamical retarding force acting on the wall, i.e., find the form of the function $F(v)$. By equating this force to the "external force" acting on the wall, we can find the dependence of the DW velocity on the external force. The applicability of this approach is due to the weakness of the relaxation in the magnetic material, and can be justified by the inequality $g(\Delta H) \ll \omega_0$, where (ΔH) is the magnetic resonance line width and ω_0 is the resonance frequency. This condition is fulfilled in the majority of magnetic materials.

The external force acting on a unit area of the DW is equal to the difference between the energies of the phases "to the right" and "to the left" of the wall, and is directed to the side of the more favored phase. In the simplest case, when the DW separates domains of two phases with a magnetization jump equal to $\Delta\mathbf{M}$ and the same energy in zero field, the strength of the magnetic pressure $P_H = \mathbf{H}\Delta\mathbf{M}$. For DW in WFM the expression for P_H can be reduced to the form

$$P_H = \frac{4M_0 d}{\delta} H. \tag{3.10}$$

In writing down (3.10), we assumed that the external field

H is parallel to the equilibrium direction of **m**.

The computation of the retarding force $F(v)$ is a significantly more complicated problem (see Refs. 102–105). The point is that the relaxation phenomena in magnetic materials require a microscopic treatment, and cannot always be described in a phenomenological fashion. Allowance for the relaxation is often made by adding relaxation terms to the Landau-Lifshitz equations, or by introducing a phenomenological dissipation function that depends on one relaxation constant. The value of this constant is taken, for example, from magnetic-resonance experiments.

In the description of DW motion in a magnetic material, this approach is only qualitatively applicable. The point is that, first, a magnetic material is a medium with strong spatial and temporal dispersion, and even in the case of small magnetization oscillations the dissipation, which is determined by the imaginary part of the magnetic susceptibility, cannot be described by a single phenomenological constant (see Ref. 17, §31). Second, the DW-induced deviations of the magnetization are not small, and are not determined only by the linear susceptibility. Finally, an important contribution to the retarding force acting on the DW is made by the processes of Cherenkov emission of quasiparticles (e.g., phonons). The contribution from these processes leads to the appearance of sharp peaks in the $F(v)$ curve at DW velocity values close to the phase velocity of the quasi-particles.

We shall discuss the contribution of the quasiparticle-emission processes in Sec. 4. As to the description of the magnon-induced retardation we shall use the phenomenological approach (the simplest and clearest approach), taking account of the spatial dispersion by choosing a dissipation function for the magnetic material.

Let us, following Ref. 106, write the dissipation function of the magnetic material in the form

$$Q=\frac{M_0}{2g}\int \mathrm{d}\mathbf{r}\left[\lambda_r\left(\frac{\partial \mathbf{l}}{\partial t}\right)^2+3\lambda_e\left(\frac{\partial}{\partial x_i}\left[\mathbf{l},\frac{\partial \mathbf{l}}{\partial t}\right]\right)^2\right]; \quad (3.11)$$

here we have introduced relaxation constants, λ_r and λ_e, due, respectively, to the relativistic and exchange interactions. An estimate for the relation between them is

$$\lambda_e \sim a^2\lambda_r\frac{\delta}{\beta}.$$

The dissipation function determines the rate at which the energy of the system is dissipated. Using the relation $2Q=vF(v)$, we can compute the retarding force acting on a unit DW area. Substituting (3.7) or (3.8) into (3.11), we obtain for the magnon drag the expression

$$F(v)=-\frac{2vM_0}{gx_0}\left\{\frac{\lambda_r}{[1-(v^2/c^2)]^{1/2}}+\frac{\lambda_e/x_0^2}{[1-(v^2/c^2)]^{3/2}}\right\}. \quad (3.12)$$

At low velocity values $v \ll c$, this formula goes over into the usual formula for the retarding force acting on a moving DW (see Ref. 27), but with the relaxation constant λ replaced by the effective value $[\lambda_r+(\lambda_e/x_0^2)]$. The two contributions to $F(v)$ can, on the basis of the estimate for the ratio λ_e/λ_r, be expected to have the same order of magnitude (whereas only λ_r makes a contribution to the homogeneous-resonance line width). At higher DW velocities the two terms depend differently on the DW velocity, i .e., the dispersion in the magnetic material is manifested fully.

By equating the expression (3.12) for the retarding force to the expression (3.10) for the magnetic pressure, and separating out the function $v(H)$, we can obtain a theoretical curve for the dependence of the wall velocity v on the external field H. For $\lambda_e < \lambda_r x_0^2$, this procedure can be carried out analytically, and it is easy to obtain for the function $v(H)$ the expression

$$v=\frac{\mu H}{\sqrt{1+(\mu H/c)^2}}, \quad \mu=\frac{2dgx_0}{\lambda_r\delta}, \quad (3.13)$$

where μ is the DW mobility. The function $v(H)$, in the form (3.13), was first obtained in Refs. 89 and 90.

A more detailed analysis of the experimental $v(H)$ curve may enable us to determine the constants λ_r and λ_e independently. It is significant that, on the strength of the theoretical ideas, the exchange and relativistic relaxation constants should depend differently on the temperature.[17] Thus, the determination of λ_r and λ_e from the $v(H)$ curve is of interest not only for the more accurate determination of the laws governing DW retardation, but also for the investigation of the general picture of the relaxation processes that occur in magnetic materials.

Experiments on the study of the motion in the orthoferrites of DW with velocity approaching the limiting velocity, were first performed by one of the present authors (M. V. Ch.), Shalygin, and de la Campa,[61,62] and are described in Sec. 2 above. The $v(H)$ curve obtained in these experiments is in good agreement with the formula (3.13), as illustrated above by Fig. 13, which was taken from Ref. 107. The experimental $v(H)$ curve exhibits deviations from the smooth curve given by the formula (3.13). These anomalies have the form of shelves, and are due, as we have already noted, to the Cherenkov emission of quasiparticles. A theory of DW motion with allowance for this effect will be presented below in Sec. 4.

In spite of the fact that the phenomenological description of the relaxation agrees quite well with experiment, there are a number of questions, the answers to which cannot, in principle, be found in this approach. For example, it is of interest to compute the relaxation constants λ from first principles, and compare their absolute values and temperature dependences with experiment.

The problem of the computation of the DW mobility in the orthoferrites was raised in the 1970's by a number of authors (see Refs. 81 and 53b). But these authors in fact computed the lifetime of the magnons with $k=0$, and from these results they computed the relaxation constant $\lambda(T)$, which was then used, on the basis of (3.13), to compute μ. In view of the above-noted circumstances (the strong dispersion of the susceptibility of the magnetic materials and the soliton nature of the DW), the good agreement of the temperature dependence of μ with experiment achieved in this approach seems to us to be fortuitous.

In Refs. 102 and 103 a microscopic theory of DW retardation in ferromagnets is proposed which consistently takes account of the characteristics of the problem. The retardation is treated as a consequence of the interaction of the DW with the magnon thermostat. The method developed can

also be used to analyze DW retardation in the WFM. In Ref. 105 a theory of DW retardation in the orthoferrites is constructed on the basis of a microscopic approach. It is shown that at room temperatures $\mu \propto 1/T^2$, which agrees with experiment. This dependence should be replaced by $\mu \propto 1/T$ as the temperature is lowered. At $T \ll \hbar\omega_1 \sim 20$ °K, the dominant contribution to the retardation should be made by the processes of phonon scattering by the DW[108] and the interaction of the DW with defects,[109] since the magnon density n is small in this case: $n \propto \exp(-\hbar\omega_1/T)$.

The coefficient in the dependence $\mu \propto 1/T^2$ for $T \ll \hbar\omega_1$ is, in order of magnitude, equal to the experimental value.[105] A more precise quantitative comparison is difficult, since the theoretical value of the DW mobility essentially depends on a large number of crystal constants, including those that have a slight effect on the static and linear high-frequency properties of the orthoferrites.

It seems to us that the investigation of the DW mobility in high-grade single crystals over as broad a temperature range as possible is quite a pressing problem, since it will allow us to ascertain the laws governing the interaction of the magnons with the magnetic soliton describing the DW.

4. CHERENKOV EMISSION OF QUASIPARTICLES DURING THE MOTION OF A DOMAIN WALL

The first experiments on the study of DW dynamics in orthoferrites revealed the existence of anomalies, described above in Sec. 2, in the dependence of the wall velocity on the driving field. These anomalies had the form of segments with a small differential mobility (small shelves) at wall velocities close to the (longitudinal and transverse) sound velocites.[52,61]

In subsequent experiments it was established that similar anomalies (shelves) occur at other velocity values not connected with the velocities of sound[63,64,75-77]; there can be several score of such shelves (see Sec. 2). Anomalies have been observed at the sound velocities in iron borate as well.[93]

According to the theory of forced DW motion developed above, the anomalies in the dependence $v(H)$ are due to anomalies in the dependence of the retarding force F on the wall veclocity v. Specifically, when the DW velocity is close to the phase velocity of some wave in the magnetic material, there occurs intense Cherenkov emission of this wave. This radiation plays the role of an additional relaxation channel. Consequently, the form of the function $F(v)$ and, hence, that of the function $v(H)$, undergo a drastic change in a fairly narrow range of velocity values.

These ideas are used in Ref. 110 to explain the anomalies that occur in the $v(H)$ curve for the orthoferrites at DW velocities close to the velocities of sound.[6)] It is suggested in Refs. 89, 64, and 112 that the remaining anomalies may be connected with the emission of other quasiparticles, e.g., surface or optical magnons and phonons. The emission of Rayleigh phonons is theoretically considered in Ref. 113. Thus, there arises a general concept, according to which each anomaly in the $v(H)$ curve is accounted for by a definite quasiparticle branch. Within the framework of this concept, the problem of analyzing the elementary-excitation spectrum in a magnetic material on the basis of data on DW motion[89,112-114] is one that arises naturally.

a) General relationships

Let us discuss some general laws governing the Cherenkov emission of quasiparticles[112] during the motion of a DW. For this purpose let us write down the Hamiltonian for the interaction between some field u and a moving DW:

$$H_{\text{int}} = \int \mathrm{d}\mathbf{r}\, U(\mathbf{l}, \mathbf{m})\, u; \tag{4.1}$$

here u is the field operator for the corresponding field and $U(\mathbf{l}, \mathbf{m})$ is determined by the magnetization distribution in the DW. Since at points far from the DW the Hamiltonian of the system does not contain terms linear in u, we can assume that U vanishes if $\mathbf{l} = \mathbf{l}_0$ and $\mathbf{m} = \mathbf{m}_0$ ($\mathbf{l}_0$ and $\mathbf{m}_0$ are the equilibrium values of the vectors $\mathbf{l}$ and $\mathbf{m}$).

Generally speaking, H_{int} contains terms that are nonlinear in u, but it is sufficient to limit ourselves to (4.1) in our problem. We shall also assume that the field u is linear. The nonlinearity of the excited field is taken into account in Ref. 115. It turns out that under certain conditions shock waves of the u field can be excited which travel with a velocity different from the DW velocity, and move away from the wall. But this circumstance is not important for the analysis of the DW retardation.

If the field operator u is represented in the form of superposition of creation and annihilation operators for quasiparticles with momentum k, then the Hamiltonian (4.1) will describe the processes of quasiparticle emission (absorption) by the moving DW. Since the DW is a plane, the quasiparticles produced by it will have a momentum only along the normal $\mathbf{n}$ to the DW. Thus, (4.1) can be rewritten in the form

$$H_{\text{int}} = \sqrt{\frac{S}{L}} \sum_k (U_k e^{-ikvt} c_k^+ + \text{H.c.}), \tag{4.2}$$

where S is the area of the DW and L and k are the dimensions of the system, and the component of the momentum along $\mathbf{n}$. The amplitude U_k is proportional to the Fourier transform of $U_0(x) \equiv U(\mathbf{l}_0(x), \mathbf{m}_0(x))$.

Notice that we can easily gain some insight into the structure of U_k without having to specify the form of the field. Since the deviation of the magnetization in the DW is localized in a region $\Delta\xi \sim x_0$, and decreases exponentially outside this region, it is not difficult to obtain for U_k the estimate

$$U_k \sim \zeta \exp(-kx_0), \quad kx_0 \ll 1; \tag{4.3}$$

here ζ is a parameter characterizing the intensity of the interaction of the field u with the field of the magnetization. Because of (4.3), it is important that the DW interact intensely only with the long-wavelength quasiparticles, for which $k \lesssim 1/x_0$, i.e., whose wave vectors k are much smaller than the dimension of the Brillouin zone.

We shall assume that the interaction of the magnetization field with the field u is weak, i.e., that $\zeta \ll 1$. In this case the effect of the DW on the quasiparticles of the field u can easily be taken into account on the basis of (4.2) and standard perturbation theory (see Ref. 116). Let us write out the general expression for the rate $\dot{E}$ of loss of DW energy per

unit DW area:

$$\dot{E} = v \int_{-\infty}^{+\infty} k\,dk\,|U_k|^2 \delta(\omega_k - kv); \tag{4.4}$$

here ω_k is the frequency of the quasiparticle with wave vector k. The quantity $\dot{E}/2$ has the meaning of a correction, due to the interaction with the given field of the quasiparticles, to the dissipation function Q of the wall. It is easy to see that $\dot{E} \neq 0$ only in the case when the equation

$$\omega_k = kv, \quad \text{or} \quad v = v_{ph}(k) = \frac{\omega_k}{k} \tag{4.5}$$

has a real root. Thus, Cherenkov emission occurs when the wall velocity coincides with the phase velocity v_{ph} of a quasiparticle. This condition changes in the presence of defects (see Sec. 4c below).

Let us, making use of the presence of the δ function in (4.4), rewrite the expression for the dissipation function Q in the form

$$Q = \frac{v}{2} \sum_{\alpha} k_\alpha |U_{k\alpha}|^2 \left| \frac{\partial \omega}{\partial k_\alpha} - v \right|^{-1}, \tag{4.6}$$

where k_α is a real root of (4.5); the subscript "α" numbers the roots of this equation.

The possession or otherwise of roots by (4.5) affects the behavior of the quantity $\langle u \rangle$ as well. If (4.6) has no roots, and $Q = 0$, then the mean value of the field u is localized near the DW, and $\langle u \rangle$ decreases exponentially as $(\xi - vt) \to \pm\infty$. If, on the other hand, $Q \neq 0$, then the quantity $\langle u \rangle$ is nonzero on one side of the DW: $\langle u \rangle \neq 0$ for $\xi - vt \to +\infty$ and $\langle u \rangle = 0$ when $\xi - vt \to -\infty$ if $v_{ph}(k_\alpha) < v_g(k_\alpha)$ and, conversely, $\langle u \rangle = 0$ when $\xi - vt \to +\infty$ and $\langle u \rangle \neq 0$ when $\xi - vt \to -\infty$ if $v_{ph}(k_\alpha) > v_g(k_\alpha)$. Here $v_g = \partial\omega_k/\partial k$ is the group velocity of the quasiparticle. This result follows from the fact that the transfer of the field energy occurs with the group velocity. In consequence, the wave packets of the field u either are ahead of ($v_{ph} < v_g$), or lag behind ($v_{ph} > v_g$), the DW. For this quantity the case $v_{ph} = v_g$, i.e., the linear quasiparticle dispersion law, is a special case.

For nonactivation particles with a linear dispersion law of the form $\omega_k = sk$, it is, in accordance with the formula (4.6), to be expected that the peak emission will occur at $v \approx s$, i.e., the quasiparticles for which s is smaller than c also contribute to the DW-energy dissipation. This condition is satisfied by the longitudinal and transverse phonons in ortho-ferrites and in iron borate. It should, however, be noted that the situation is a special one for the quasiparticles with a linear dispersion law; for example, (4.6) is divergent when $v = s$. In this case it is necessary to take into consideration either the deviation of the dispersion law from the linear law, or the damping of these quasiparticles.[110]

b) Emission of acoustic phonons

At present only the $v(H)$ anomalies occurring at $v \approx s_t$ and $v \approx s_l$ have been reliably identified with quasiparticle emission. Therefore, let us consider in greater detail the emission of acoustic phonons.

The interaction of the magnetization field with the field of the elastic deformations is determined by the magnetoelastic energy w_{me}:

$$w_{me} = M_0^2 [f_{ik,\,lm}(l_i l_k - l_i^{(0)} l_k^{(0)}) + f'_{ik,\,lm}(l_i m_k - l_i^{(0)} m_k^{(0)})]\, u_{lm}, \tag{4.7}$$

where $\mathbf{l}^{(0)}$ and $\mathbf{m}^{(0)}$ are the equilibrium values of the vectors $\mathbf{l}$ and $\mathbf{m}$ in the homogeneous phase $\Phi_\parallel$, $u_{lm} = 1/2 \times (\partial u_l/\partial x_m + \partial u_m/\partial x_l)$ is the strain tensor, $\mathbf{u}$ is the elastic-displacement vector, and f and f' are the magneto-elastic interaction tensors. If we limit ourselves in the expression for w_{me} to only the terms containing the vector $\mathbf{l}$, then, on account of the symmetry of the orthoferrites, which belong to the group D_{2h}^{16}, that element of the tensor f which describes the interaction of a DW located in the $z0y$ plane with transverse sound propagating along the y axis will be equal to zero, i.e., $f_{ik,ly} = 0$ if i, k, and l assume the value x or z. At the same time the tensor describes the interaction of a longitudinal acoustic wave propagating along the y axis with the DW, i.e., $f_{ik,yy} \neq 0$ if $i, k = x, z$. Therefore, to describe the interaction of the DW with a transverse acoustic wave, we must include the $\mathbf{m}$-dependent magnetostriction energy. Among the nonzero elements of the tensor f' are elements of the type $f'_{ik,ly}$: for $l = x, z$ these are $f'_{xy,\,yz}$ and $f'_{zy,xy}$. Thus, the interaction of the DW with transverse sound is described by the energy

$$w'_{me} = M_0^2 m_y (f'_{xy,\,yz} l_{0x} n_{yz} + f'_{zy,\,xy} l_{0z} u_{xy}), \tag{4.8}$$

where $\mathbf{l}_0$ is the value of the vector $\mathbf{l}$ in the DW. Since the quantity m_y is proportional to the DW velocity [see (3.7)], w'_{me} will also be proportional to this velocity.[125]

Replacing $\mathbf{l}_0(x)$ and m_y by their distributions in the DW and u_{ik} by its expression in terms of the phonon creation and annihilation operators, we obtain a Hamiltonian of the form (4.2). Naturally, the amplitudes of this Hamiltonian depend on the phonon polarization, so that, instead of U_k, we should write $U_\lambda(k)$. The structure of these amplitudes for ac-type DW can be schematically written in the form

$$\begin{gathered} U_l(k) = f_l g_1[x_0(s)\,k], \\ U_t^x(k) = \frac{v}{c} f_t^x g_1[x_0(s)\,k], \quad U_t^z = \frac{v}{c} f_t^z g_2[x_0(s)\,k], \end{gathered} \tag{4.9}$$

where the f's are the effective magnetostriction constants, $f_i \sim \beta$,

$$g_1(x_0 k) = \frac{\pi k x_0^2(s)}{\operatorname{sh}[\pi k x_0(s)/2]}, \quad g_2 = \frac{\pi k x_0^2(s)}{\operatorname{ch}[\pi k x_0(s)/2]}. \tag{4.10}$$

The dissipation function describing the transfer of energy from the DW to the phonons is given by the formula (4.6), in which we must sum over the phonon polarization and take as k the roots of Eq. (4.5). To determine the roots k_0 of this equation, let us represent the phonon dispersion law in the form

$$\omega_\lambda(k) = s_\lambda k\,[1 - \sigma_\lambda (ak)^2]. \tag{4.11}$$

The coefficient σ_λ determines the deviation of the dispersion law from the linear law. The values $k_{0\lambda}$ are then given by the formula

$$k_{0\lambda} = \frac{s_\lambda - v}{a\sigma_\lambda s_\lambda}. \tag{4.12}$$

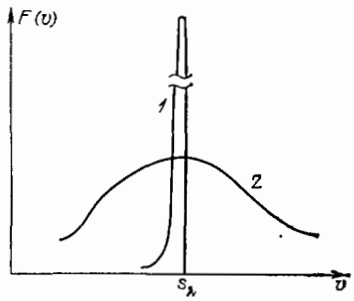

FIG. 20. Dependence of the strength of the phonon drag on the domain wall velocity. 1) Weak phonon attentuation; 2) strong phonon attenuation.

The dependence of the dissipation function on the DW velocity is governed largely by the functions $g_\lambda[x_0k_0]$. Indeed, when $k_0x_0 \gg 1$, i.e., when the inequality $|s_\lambda - v| \gg \sigma s_\lambda (a/x_0)^2$ is satisfied, the quantity Q_λ is exponentially small: $Q_\lambda \propto \exp[-2|s_\lambda - v|x_0^2/\sigma a^2 s_\lambda]$. Consequently, when the phonon attenuation is ignored, the phonon drag is substantial only in a narrow range of velocity values (see the curve 1 in Fig. 20):

$$\Delta v = s_\lambda - v < \sigma_\lambda s_\lambda \left(\frac{a}{x_0}\right)^2 \sim 10^{-4} s_\lambda. \tag{4.13}$$

Within this range the phonon drag F_λ is quite large. Estimating its maximum value from the formula $F_\lambda = 2Q_\lambda / v$, we find that for a Bloch wall

$$F_l^{\max} \sim \zeta_l f_l M_0^2,$$
$$F_{tx,z}^{\max} \approx \zeta_l f_t \left(\frac{s_t}{c}\right)^2 M_0^2, \quad \zeta_\lambda = \frac{f_\lambda M_0^2}{\rho_0 s_\lambda^2}. \tag{4.14}$$

The quantity ζ_λ is a small dimensionless magnetoelastic coupling constant. Using the standard values[25] $fM_0^2 \sim 3\times 10^7$ erg/cm^3 and $\zeta \sim 10^{-5}$, we obtain for $F^{\max}$ the estimate: $F_l^{\max} \sim 10^7$ dyn/cm^2. Because of the presence of the small factor $(s_t/c)^2 \approx 0.05$, the value of $F_t^{\max}$ is smaller: $F_t^{\max} \sim 5\times 10^5$ dyn/cm^2. In the case of a Bloch DW only the terms containing m_x, $m_y \propto (v/c)$ contribute to F_t. If we ignore the effect of the motion-induced structural change in the DW, then we find the $F_t = 0$ (Refs. 110 and 117). the fact that F_t is smaller in magnitude than F_l is clearly revealed in experiments on Bloch-DW motion (see Sec. 2 above). Let us note that if in an experiment the DW turns out to be inclined to the a–c plane, then the value of F_t turns out to be much higher.[117].

When phonon attenuation is taken into account, the phonon drag mechanism remains qualitatively the same, but the quantitative values of $F_{\max}$ and the velocity interval Δv change appreciably. Allowance for the attentuation can be adequately made at the phenomenological level by "smearing" out the δ function in the formula (4.6):

$$\delta(\omega) \to \frac{1}{\pi} \frac{\Gamma(\omega)}{\omega^2 + \Gamma^2(\omega)}, \tag{4.15}$$

where $\Gamma(\omega)$ is the phonon line width, which can be expressed in terms of the viscosity of the crystal:

$$\Gamma(\omega) = \frac{\eta}{2}\omega^2 \equiv \gamma k^2. \tag{4.16}$$

The experimental η value for the orthoferrites at room temperature is of the order of 10^{-11} sec, i.e., $\gamma \sim 1$ cm^2/sec. We can, by analyzing (4.4) with allowance for the substitutiton (4.15), easily show that the phonon attenuation is appreciable when $\gamma > \gamma_c = \sigma(sx_0)(a/x_0)^2 \sim 10^{-4}$ cm^2/sec. This condition is fulfilled in orthoferrites at room temperatures.

If $\gamma > \gamma_c$, then $Q(v)$ is given by the interpolation formula[110]

$$Q(v) = \frac{3v}{4}\zeta f M_0^2 \frac{sx_0\gamma}{\gamma^2 + [7x_0^2(s-v)^2/2]}, \tag{4.17}$$

i.e., $F(v)$ has the form of a Lorentzian peak with the maximum at $v = s_\lambda$ (see the curve 2 in Fig. 20). Consequently, in the situation with strong sound attenuation the $F(v)$ peak is symmetric, and the decrease at the wings occurs in a power-law fashion.

The maximum value of $F(v)$ decreases with increasing γ like $1/\gamma$:

$$F^{\max} \sim \frac{3s^2}{4\gamma}\zeta f x_0 M_0^2, \tag{4.18}$$

while the width of the peak is given by the relation

$$\Delta v = |s_\lambda - v| \sim \frac{\gamma}{x_0}$$

and increases with increasing γ. For an *ac*-type Bloch wall in $YFeO_3$ at room temperature we find

$$F_l^{\max} \approx (1-10)\cdot 10^2 \text{ dyn/cm}^2$$
$$F_t^{\max} \approx (0.5-5)\cdot 10 \text{ dyn/cm}^2 \frac{s_\lambda - v}{s_\lambda} \sim 10^{-1}.$$

The investigation of the retardation of the other types of walls can be carried out in much the same way.[117] An important point here is the fact that, for the majority of the DW, including the intermediate-type DW, the expression for F_t does not contain the small factor $(s_t/c)^2$ that occurs in the case of the Bloch DW. For these DW the widths of the anomalies at $v = s_t$ and $v = s_l$ are of the same order of magnitude.

The value of the DW velocity is found by equating the retarding force to the strength of the magnetic presssure:

$$Bv + F(v) = 2m_0H. \tag{4.19}$$

Using the $F(v)$ curve (see Fig. 20), we can solve this equation graphically. The form of the function $v_0(H)$ depends essentially on the relation between the mobility coefficient B and the amplitude of the function $F(v)$. If $B + (dF(v)/dv) > 0$ (low wall mobility), then the function $v_0(H)$ is single-valued (see the curve 2 in Fig. 21). This curve clearly exhibits a region of low differential mobility (a shelf). We can, in accordance with (4.19), estimate the width of this shelf:

$$\Delta H \approx \frac{F^{\max}}{2m_0}. \tag{4.20}$$

Since $m_0 \sim 10$ G for $F^{\max} \sim 10^2$–10^3 dyn/cm^2 we obtain $\Delta H \sim 10$–100 Oe. The characteristic shelf widths observed in experiments on intermediate-type-DW dynamics at room temperatures are 30 Oe for $YFeO_3$ and 100 Oe for $TmFeO_3$. In line with the fact that $F^{\max}$ for transverse sound and the Bloch DW is smaller than for longitudinal sound, the experi-

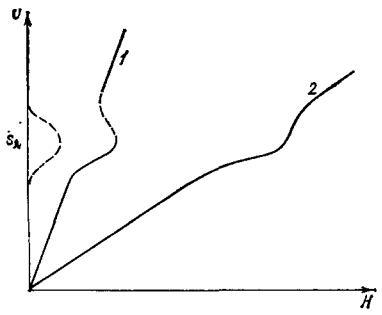

FIG. 21. The $v(H)$ curve for the domain wall when allowance is made for the phonon drag (schematic). 1) High mobility: nonunique dependence; 2) low mobility: unique dependence. The dashed line in curve 1 corresponds to the regions of instability of the straight domain wall.

mentally observed shelf width at $v = s_t$ is smaller than the width observed at $v = s_l$. This rule was revealed in experiments (Fig. 22). For the remaining types of DW the widths of these shelves are of the same order of magnitude, which is in accord with the theory expounded above.

When the mobility μ or the value of $F^{\max}$ increases, the condition $B + (dF(v)/dv) > 0$ may be violated in the region where $F(v)$ decreases. In this case there arises at velocity values satisfying the condition

$$B + \frac{dF(v)}{dv} < 0, \tag{4.21}$$

a region of field intensities H where the function $v_0(H)$ is multivalued (see the curve 1 in Fig. 21). According to the general nonlinear-dynamics laws (see Ref. 118), to this region corresponds a region, indicated by the dashed line in Fig. 21, of instability of the uniform motion of a straight DW. This instability manifests itself experimentally as essentially nonstationary motion of the DW. The laws governing such motion will be discussed in the following section.

c) Emission in an inhomogeneous crystal

Real samples of magnetic materials always contain inhomogeneities of various types: both random (defect clusters, dislocation pile-ups, etc.) and regular quasiperiodic inhomogeneities of growth origin. As shown in Ref. 109, the conditions for quasiparticle emission are much less rigid in an inhomogeneous crystal. In particular, the emission is possible at any DW velocity, and there arises the possibility of emission of surface magnons (SM), i.e, magnons localized near the DW, and having the linear dispersion law $\varepsilon(k_\perp) = \hbar c k_\perp [1 - (v^2/c^2)]^{-1/2}$ [see (3.11)].

The physics of this phenomenon is as follows. In a perfect crystal a quasiparticle can acquire from the DW only the momentum $\hbar\mathbf{k} = \hbar k \mathbf{e}_\xi$, where $\mathbf{e}_\xi$ is the unit vector along the normal to the DW, and the energy $\hbar\omega = \hbar k_\xi v$ [see (4.4)–(4.6)], which leads to the rigid condition (4.5). In the presence of inhomogeneities the transfer of additional momentum $\mathbf{q}\hbar$ from an inhomogeneity is possible. For this to be possible, the Fourier expansion of the inhomogeneity should contain the term $\Phi_q \exp(i\mathbf{q}\cdot\mathbf{r})$. The law of conservation of energy and momentum in an elementary act of quasiparticle emission can be written in the form $\varepsilon(\mathbf{q} + k_\xi e_\xi) = \hbar k_\xi v$, and, for any v, this conservation law can be satisifed by an appropriate choice of $\mathbf{q}$.[109] In particular, in the emission of a SM the component q_ξ is transferred to the DW, while $\mathbf{q}_\perp$ is transferred to the SM, and the conservation law has the form $\varepsilon(\mathbf{q}_\perp) = \hbar v q_\xi$, where $\mathbf{q}_\perp$ is the component of $\mathbf{q}$ in the plane of the DW. Accordingly, the retarding force stemming from the SM emission has the form [see Ref. 109, formula (10) with $\varepsilon(k_\perp) = \hbar c k_\perp (1 - v^2/c^2)^{-1/2}$

$$F(v) = 2\pi \sum_q |\Psi_q|^2 q_\xi \delta\left(\frac{c|\mathbf{q}_\perp|}{\sqrt{1-(v^2/c^2)}} - v q_\xi\right); \tag{4.22}$$

here Ψ_q is the amplitude of the SM emission in the presence of inhomogeneities. If we assume that the defects are distributed randomly, and that the crystal is infinite, then (4.22), after being averaged over the defects, yields the monotonic function $F(v) = F_0 + Dv^2$. The quantity F_0 determines the contribution of this process to the coercive force.[109] The DW motion can become unstable when $D < 0$ (see the estimate in Ref. 109).

It is pointed out in Ref. 124 that, if we assume that the inhomogeneity is periodic, but the crystal is finite, then the SM excitation can occur at some selected discrete set of DW velocities. Let us discuss this phenomenon in greater detail.

We shall, following Zvezdin and Popkov,[124] assume that the inhomogeneity in the crystal is periodic, with period $2\pi/q_\xi$, in the direction of motion of the DW (i.e., along the ξ axis). Furthermore, let us, in accordance with the Zvezdin-Popkov model,[124] assume the presence of an inhomogeneity of any kind along the normal to the surface of the platelet (the ξ axis). If we denote the platelet thickness by l, then the SM wave vector in (4.22) may assume the discrete values $q_\xi^{(n)} = \pi n/l$, where n is an integer. For a SM with a given n to be emitted, it is necessary that the Fourier expansion of the inhomogeneity along the ζ axis contain the term $\exp(i\pi n_\xi / l)$.

It follows from the conservation law in (4.22) that, in the model in question, the emission of a SM is possible when

$$c\frac{\pi n}{l}\left(1 - \frac{v^2}{c^2}\right)^{-1/2} = q_\xi v,$$

i.e., when $v = v_n$, where v_n is given by the formula[124]

$$v_n = c\frac{\pi n}{q_\xi l}\left[1 + \left(\frac{\pi n}{q_\xi l}\right)^2\right]^{-1/2}. \tag{4.23}$$

Thus, if there exists in the crystal a system of three-

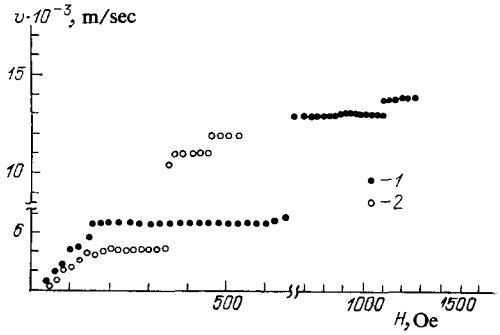

FIG. 22. Magnetoelastic anomalies on the $v(H)$ curve for the Bloch (1) and Néel (2) domain walls in a $YFeO_3$ sample of thickness 25 μm.[76]

dimensional inhomogeneities that are periodic over the plane of the platelet, then flexural vibrations of the DW will be excited during the motion of the wall with a velocity belonging to some discrete set of velocity values v_n. As a result, the retarding force increases, and anomalies of the shelf type appear in the $v(H)$ curve, when $v \approx v_n$. This is apparently the only mechanism that allows us at present to explain the experiments (see Sec. 5 and Fig. 26 there) in which more than 10 such shelves were observed. The question of the origin of the inhomogeneities of the requisite type, however, remains open.

5. NON-STEADY-STATE NON-UNIDIMENSIONAL DOMAIN WALL MOTION

The experimental $v(H)$ curve for certain DW moving with supersonic velocities (see Figs. 15 and 17) reveals the existence of a velocity instability region that manifests itself in a strong straggling of the transit times of the DW. It is natural to relate this instability with the instability of the uniform DW motion in the region of negative differential mobility (see Fig. 21 in Sec. 4).

Let us investigate the non-one-dimensional motion of a DW, treating the wall as a membrane with surface energy σ and mass m_*.[119] The equation for the wall displacement $f(x, z, t)$ with allowance for the driving force P_H and the drag (let us recall that $c^2 = \sigma/m_*$) has the form

$$\frac{\partial^2 f}{\partial t^2} - c^2\left(\frac{\partial^2 f}{\partial x^2} + \frac{\partial^2 f}{\partial z^2}\right) = \frac{B}{m_*}\left(\mu H - \frac{\partial f}{\partial t}\right) - \frac{1}{m_*} F\left(\frac{\partial f}{\partial t}\right); \tag{5.1}$$

here μ is the DW mobility, $B = 2m_0/\mu$, and $F(v)$ is the phonon drag. Let us consider small deviations from the steady-state solution, i.e., let us set $f = vt + \varphi$. For φ we obtain[117,118]

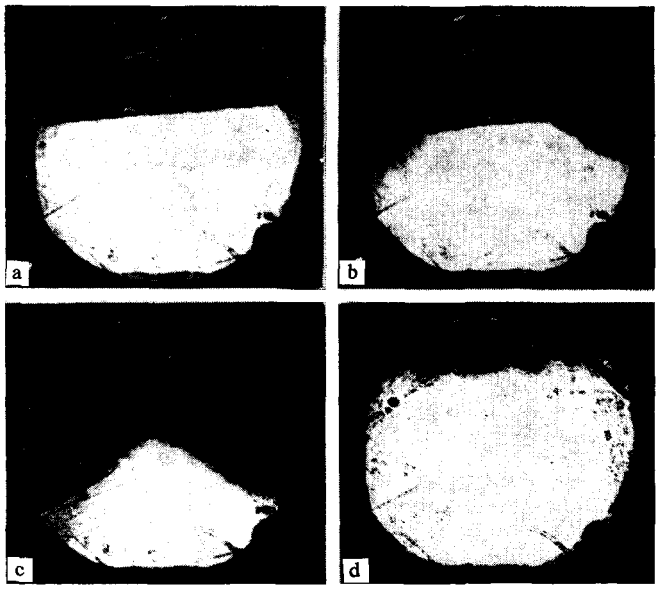

FIG. 23. Single-shot high-velocity photographs of the dynamic domain structures in $YFeO_3$ in a 140-Oe magnetic field, taken at 20-nsec intervals (a–c), and in a 2300-Oe magnetic field (d).[74]

$$\varphi \sim (\exp \gamma t + i\mathbf{k}_\perp \mathbf{r}_\perp), \quad \gamma = -\nu(v_0) \pm \sqrt{\nu^2(v_0) - c^2\mathbf{k}_\perp^2}, \tag{5.2}$$

where $\nu = B + dF(v)/dv$. From this it follows that, when $\nu(v_0) < 0$, φ increases exponentially in time, and uniform motion is unstable.

Let us estimate the values of the parameters of the magnetic material at which the inequality (4.21) can be satisfied, and instability can develop. It is easy to see that this inequality is satisfied at sufficiently small values of B, i.e., at large values of the mobility, specifically, when $\mu > \mu_c$, where

$$\mu_c = 2m_0\left(\max\left|\frac{dF(v)}{dv}\right|\right)^{-1} \approx \frac{2m_0\Delta v}{F_{max}}; \tag{5.3}$$

here Δv and F_{max} are characteristics of the phonon peak and m_0 is the magnetization of the WFM. In the linear approximation the DW inhomogeneity grows exponentially in time. It is clear that the exponential increase of the deviation of the shape of the wall from the rectilinear shape will be stopped by the nonlinearity of the system. This regime of DW motion has thus far not been theoretically analyzed; therefore, the experimental investigation of the developed DW-motion instability is especially urgent. In a number of investigations[74–76] this regime of wall motion was investigated by the method of high-speed photography, which made it possible to obtain information about the shape of the moving DW in an orthoferrite. It was shown in these investigations[74–76] that a solitary, straight, intermediate-type DW in an yttrium orthoferrite platelet does not change its rectilinear form right up to the velocity of transverse sound. Upon further increase of the driving pulsed field, the shape of the moving DW changes when the motion becomes supersonic.[72,74] There appear on the wall semispherical leading sections whose velocities can be significantly higher than the velocity of sound. The higher the DW mobility in the sample under investigation is, the more pronounced are the indicated leading sections. In $YFeO_3$ samples, which were investigated in the experiments indicated above,[74–76] a maximum mobility of 2×10^4 cm/sec-Oe is attained at a temperature of 110 °K. The high-speed dynamic-domain-structure photographs shown in Fig. 23 were taken at this temperature. The radius of curvature of the leading sections varies from several hundred to 120 μm as H is varied from 120 to 2650 Oe.

On passing through the sound velocity the DW changes its apparent width. Two to three nanoseconds after passing through the sound velocity the DW broadens sharply and becomes inhomogeneous and non-one-dimensional.[76] Ten to fifteen nanoseconds after this the DW straightens, and its apparent width decreases (Fig. 24).[77,120] The time intervals indicated above are comparable to the relaxation time in yttrium othoferrite.

The leading sections appear at random places, and do not, as a rule, recur at the same places from time to time. Figure 25 shows a series of twin dynamic domain structures in $YFeO_3$, obtained during one passage of the DW through a sample cut perpendicular to the optic axis. In a 127-Oe magnetic field the central part of the DW remains straight and moves with the velocity of transverse sound, the leading sections occurring at places closer to the edges. The positions of these sections change from time to time (see Fig. 25). Final-

FIG. 24. Domain wall in the process of surmounting the sound barrier in $YFeO_3$ at 110 °K.[77] The time interval between two consecutive photographs is ~2 nsec.

ly, in high fields virtually the entire DW moves with constant velocity, which is indicated by the constancy of the form of the dynamic domain structures obtained at 5- and 15-nsec time intervals. In Fig. 25 the dark band shows the region traversed by the DW during the indicated time interval.[76,77] The process of formation of leading sections and the modification of the shape of the moving orthoferrite DW constitute a DW self-adjustment that becomes more and more stable as H increases. The point of intersection of neighboring leading sections have velocities that are higher by a factor of $1/\cos(\alpha/2)$, where α is the angle at the singular point of the DW. The DW curvature, on the other hand, also facilitates the straightening of the wall with time. For these two reasons the DW straightens in the course of its motion.

Thus, the orthoferrite DW ceases to be a one-dimensional object on going through the sound velocity limit. The experimental data on supersonic DW motion indicate the necessity of the development of a theory of non-one-dimensional, non-steady-state DW dynamics in orthoferrites.

The existing one-dimensional DW-dynamics theory explains the initial stage of the development of the one-dimensional-DW instability during supersonic motion. As can be seen from the formula (5.3), the higher the DW mobility is, the stronger should be the experimentally observed instability of the wall. The results of the experimental investigation

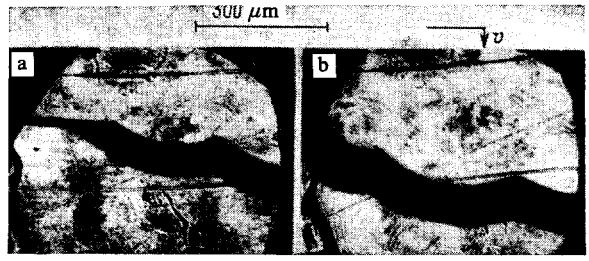

FIG. 25. Photographs of two dynamic domain structures in $YFeO_3$ at 110 °K in the course of one passage of the domain wall through the sample.[77] The dark bands are the regions traversed by the DW during the time interval (5 nsec) between two consecutive light pulses in 160-Oe (a) and 750-Oe (b) magnetic fields.

are as follows: when $\mu < 10^3$ cm/sec-Oe the instability practically does not occur, but at $\mu \sim 20\times 10^3$ cm/sec-Oe, which corresponds to $T = 110$ °K, there occurs a strongly pronounced instability consisting in the occurrence of a kink in the wall and the motion of the various wall sections with different velocities.[75,77]

The theoretical estimate obtained for μ_c from (5.3) with $\Delta H = 30$ Oe, $F_{max} = 2m_0\Delta H$, $\Delta v = 0.1 s_t \approx 2\times 10^4$ cm/sec is $\mu_c \approx 10^3$ cm/sec-Oe. This value agrees in order of magnitude with the experimental value. Thus, it can be assumed that the existing theory can elucidate the mechanism underlying the onset of the instability, i.e., the linear phase of the development of the DW-motion instability at velocities close to the velocity of sound.

Experiment shows that the nonlinear phase of the nonstationary motion is characterized by large-scale inhomogeneities with characteristic dimensions of the order of the dimensions of the orthoferrite domains. The nonstationary processes leading to the development of this instability necessitate the analysis of the essentially nonlinear equation (5.1) with allowance for the inhomogeneities along the x and z axes (it is possible that the modification of the shape of the moving DW begins with a depression in thickness of the wall).

From a sequence of twin dynamic domain structures similar to those shown in Fig. 25 we can determine the velocity for the stationary DW motion in orthoferrites with an accuracy higher than the accuracies achieved with all the methods employed earlier. This type of investigation has been carried out for a number of orthoferrites over a broad range of temperatures.[77]

Figure 26a shows the $v(H)$ curve at 290 °K for a DW of the intermediate type in a 120-μm-thick $YFeO_3$ platelet cut perpendicular to the optic axis. In the region below the transverse-sound velocity the character of the dependence $v(H)$ duplicates the analogous dependences obtained with the aid of the other techniques. In the 70–150-Oe region the DW velocity is constant and equal to the transverse-sound velocity. At higher H the DW velocity becomes equal to the velocity of longitudinal sound. After this, in the region of still higher H the DW moves with a velocity that takes on discrete values, the transition from one velocity to another occurring quite abruptly. About ten such velocities can be

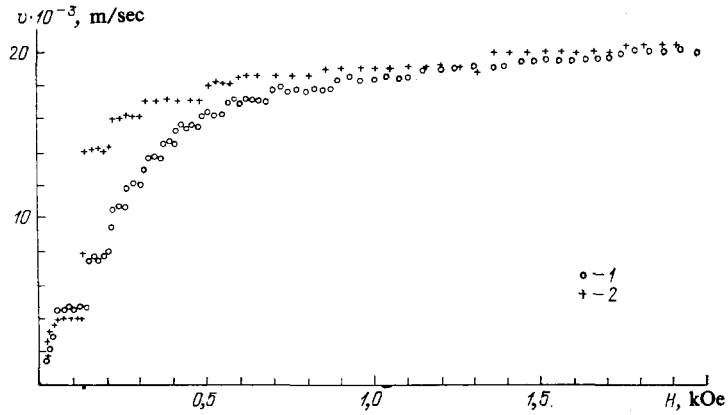

FIG. 26. Magnetic field dependence of the domain wall velocity in $YFeO_3$ at 290 °K (1) and 110 °K (2).[77]

seen in Fig. 26. These anomalies were first observed in the expriments reported in Refs. 63 and 64. The number of regions of constancy of the DW velocity in the interval from the longitudinal-sound velocity depends on the thickness of the orthoferrite platelet.

Similar experimentally observed anomalies are reported and discussed in Ref. 114. In the experiment in question the dynamics of DW under the action of a strong high-frequency field was investigated.

It is at present not clear which quasiparticle emission is the cause of the anomalies that occur at velocities higher than the velocity of sound but lower than the limiting velocity. In Ref. 76 the occurrence of these anomalies is attributed to the emission of Lamb waves. But subsequent experiments performed on platelets immersed in H_2O and CCl_4 showed that the $v(H)$ anomalies have practically the same form,[77] which raises difficulties for such an interpretation. It is possible that some of the $v(H)$ anomalies are due to the excitation of optical phonons or excitons. But it seems to us that these anomalies can most naturally be explained within the framework of the mechanism of surface-wave excitation on the DW in the presence of periodic inhomogeneities (see Sec. 4c). The set of velocities v_n, (4.23), allows us to describe satisfactorily the experiment in the range of $2\pi/q_\xi$ values from ~ 10 to $40\,\mu$m. This interpretation is complicated by the fact that there are no data on the inhomogeneities in the samples used.

Figure 26 shows the $v(H)$ curve at 110 °K for a 100-μm-thick $YFeO_3$ sample cut perpendicular to the optic axis. The transition to the supersonic velocity occurs very abruptly here. The DW velocity changes abruptly from 4 to 14 km/sec in a very narrow range of magnetic-field intensities. This is due to the very high DW mobility, which can attain a value of 2×10^4 cm/sec-Oe. As H increases further, the DW velocity assumes constant values in several regions before going over to the limiting value, which remains constant right up to the highest attainable magnetic field intensities, which range from 3 to 5 kOe, depending on the experimental conditions. It should be noted that the samples continued to have a two-domain structure right up to the indicated fields in all the cases in which they underwent thorough chemical polishing. The superlimiting velocities observed earlier with the aid of the method involving the measurement of the time of passage of the DW over a given distance between two light spots[63] were due to the appearance of new domains (which can be interpreted as localized perturbations of the magnetization field) in the region in front of the moving DW in not too thoroughly polished samples.

A similar simulation mechanism of DW motion with a "superlimiting" velocity was first proposed in Ref. 89, and was called there the soliton mechanism. It is important for its explanation that the wall divide the phases $\Phi_{\uparrow\uparrow}$ and $\Phi_{\uparrow\downarrow}$, in which the magnetization $\mathbf{m}_0$ is parallel and antiparallel to the external field $\mathbf{H}$. When $\mathbf{H}\neq 0$ the phase $\Phi_{\uparrow\downarrow}$ is metastable. Because of this a nucleation center of the stable $\Phi_{\uparrow\uparrow}$ phase can be created in the $\Phi_{\uparrow\downarrow}$ phase at some moment t_0.

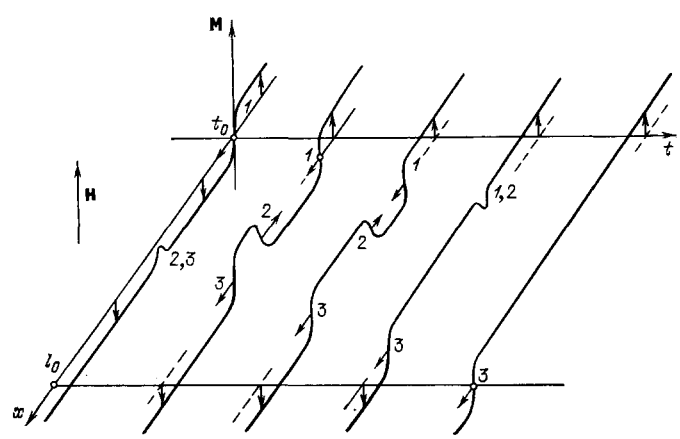

FIG. 27. Schematic representation of the soliton mechanism of simulation of the superlimiting domain wall motion.[89]

This nucleation center can have the shape of a plane or cylindrical dynamic domain (magnetic soliton). The production of the soliton can occur (fluctuationally or on a defect) within the domain, or else it can be stimulated by the leading edge of the DW. In the latter case the soliton will be created in the vicinity of the DW.

The subsequent evolution of the system is clear from Fig. 27. The created soliton does not possess a topological charge, since it contains two DW's of opposite signs. Under the action of an external field the soliton grows and becomes deformed. The DW's then move in opposite directions. One of them, labeled by the number 2 in Fig. 27, moves backwards and undergoes mutual annihilation with the original DW, labeled by 1. The second DW, labeled by 3, moves forward, and can be detected at the point of observation l_0. It is clear that this DW will arrive at the point of observation faster than the original DW would have. Thus, even if the velocity of each DW does not exceed c, the speed of "signal transmission" by the moving wall can be significantly higher than c. If in an experiment we record the crossing of a given point by the DW, then the soliton mechanism can simulate the motion of a DW with velocity higher than c. Such a mechanism of DW translation has been observed by the method of high-speed photography in ferrite-garnets.[121]

In very strong fields, in which the $\Phi_{\uparrow\downarrow}$ phase is absolutely unstable, the velocity c is not the limiting velocity, and true superlimiting DW motion is, in principle, possible.[91,112] The front of the DW is then unstable,[91] and, moreover, DW motion with $v > c$ is accompanied by Cherenkov emission of magnons.[112] For orthoferrites the corresponding field is of the order of several score kilo-oersted, and no measurements in pulsed fields of such intensity have thus far been carried out.

Nonstationary supersonic DW motion can be accompanied by a specific complication of the wall structure. At 110 °K there can propagate along a DW moving with the velocity of transverse sound in $YFeO_3$ a kink whose velocity can be as high as 20 km/sec.[122] The process of formation and motion of a kink is illustrated in Fig. 28. This figure shows photographs, taken with a 5-nsec time interval between the light pulses, of a twin dynamic domain structure in a $YFeO_3$ platelet located in a magnetic field of intensity 121 Oe. The DW has, as it goes through the transverse-sound velocity limit, a shape that is normal for the instability region. Upon a further increase of H the character of the DW motion changes abruptly. The velocity of the right semispherical part of the DW decreases sharply from 14 to 4 km/sec, while the left part of the DW still continues to move with a velocity of 4 km/sec. There appears on a DW moving with the velocity of transverse sound a kink that moves from right to left with a velocity of 20 km/sec. Figure 28 shows the successive positions of the kink at 5-nsec intervals. The time interval between two consecutive frames is ~ 3 nsec.

The formation of a kink can be explained by taking account of the field inhomogeneity inthe sample. As described in Sec. 2, a solitary DW is produced in a sample with the aid of a gradient magnetic field, as a consequence of which the resultant field acting on the moving DW decreases. A DW moving steadily with a velocity of 14 km/sec then finds itself again in a magnetic field corresponding to its non-steady-state motion, its velocity decreases to 4 km/sec, and the motion becomes a steady-state one with velocity equal to the velocity of transverse sound. If this process occurs nonuniformly in the DW plane, than a kink is produced. The adequacy of this mechanism is borne out by the fact that the amplitude of the kink decreases with increasing ∇H. On the whole, a DW with a kink is a complicated dynamical formation with a mass that varies along the length of the wall. The velocity of the kink is bounded from above by the velocity of the flexural waves on the DW, a velocity which coincides with the spin-wave velocity c on the linear section of the spectrum and with the limiting velocity for the DW motion. Thus, this velocity plays the decisive role in the dynamics of both the DW itself and the kink that propagates along it. The formation and motion of a kink on the DW confirms the existence of a discrete set of velocities for the stationary supersonic motion of the DW. The formation of kinks on moving orthoferrite DW should occur in other transitions from one steady-state velocity to the next.

CONCLUSION

The results presented in this review of experimental and theoretical investigations of nonlinear DW dynamics in WFM demonstrate the generality of the laws governing DW dynamics in different WFM and an essential difference between DW dynamics in WFM and DW dynamics in ferromagnets, e.g., in ferrite-garnets. The investigation of DW dynamics in WFM revealed for the first time supersonic DW motion under conditions of Cherenkov emission of sound, the existence of regions of instability of rectilinear DW motion, the formation of kinks on DW, and quasirelativistic DW dynamics with a limiting velocity equal to the phase velocity of the spin waves.

Let us briefly formulate some problems that are, from our point of view, of greatest interest for further research. These are, first and foremost, experimental and theoretical

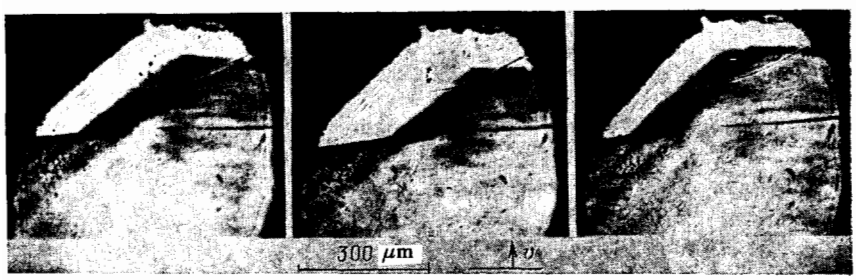

FIG. 28. Photographs of three consecutive positions of a kink on a domain wall in $YFeO_3$ at 110 °K, taken at 5-nsec intervals.[122] The time interval between two consecutive photographs is ~ 3 nsec.

investigations of the unstable motion of DW both at velocities close to the velocity of sound and at velocities in the neighborhood of the limiting velocity. The latter instabilities should develop in magnetic fields of higher intensities than those that have been used to date.

It is of interest to carry out a detailed analysis of the relaxation processes. To obtain information about the internal processes, we must perform experiments over a broad range of temperatures and use more perfect single crystals. Of no less interest is the study of the interaction of moving DW with inhomogeneities, for which purpose a crystal with a controllable defect structure should be used.

The combination of high transparency, large Faraday rotations, high mobilities, and record-high DW velocities makes the WFM promising materials for construction of the devices of the type of optical shutters, space-time light modulators, and other devices for the optical processing of information.

[1)]Active research into other types of materials with mobile domains is going on at present. Among these materials are amorphous metallic films containing rare-earth metals and ferrite films with submicron domains. But the experimental data on these materials are considerably less complete, and we shall not discuss them below.

[2)]This approximation does not hold in a narrow neighborhood of the compensation point for the mechanical moments of ferrite sublattices.[19]

[3)]It should be noted that the presence in a garnet of strong anisotropy in the basal plane, or of a strong field in the plane of the wall can, apparently, hinder the formation of inhomogeneities in the plane of the DW, in virtue of which the one-dimensional Walker model provides a better description of the DW dynamics, (Ref. 12, p. 77).

[4)]It is worth noting that, if for $\xi \to +\infty$ and $\xi \to -\infty$, the same values of $\mathbf{m}$ correspond to the wall and only the $\mathbf{l}$ values differ, then such a wall in not topologically stable, and can be annihilated. For this purpose it is sufficient to create in the DW plane a ring disclination (a line of discontinuity of the vector $\mathbf{l}$), and then increase the radius of the ring.[31] The potential barrier that must be surmounted in this process is finite. Such a situation is characteristic of antiferromagnets without weak ferromagnetism.

[5)]As recently shown in Ref. 123, the limiting DW velocity in a WFM with an odd principal axis may be determined by the relativistic interactions, and may differ essentially from c.

[6)]A similar problem is discussed in Ref. 111 for a ferromagnet and from a somewhat different standpoint.

[1]S. V. Vonsovskiĭ, Magnetizm (Magnetism), Nauka, M., 1971 (Engl. Transl., Halsted, N. Y., 1975).
[2]P. Weiss, J. Phys. Radium **6**, 661 (1907).
[3]F. Bloch, Z. Phys. **74**, 295 (1932).
[4]L. D. Landau and E. M. Lifshitz, Sov. Phys. **8**, 153 (1935), also in: L. D. Landau, Sobranie trudov, Vol. 1, Nauka, M., 1972 [Engl. Transl., Collected Papers, Gordon & Breach, N. Y., 1965, p. 254].
[5]L. Néel, Cahiers de Phys. No. 25, 1 (1944).
[6]H. Barkhausen, Z. Phys. **20**, 401 (1919).
[7]F. Bitter, Phys. Rev. **38**, 1903 (1931).
[8]N. S. Akulov and M. V. Dekhtyar, Ann. Phys. (Leipzig) **15**, 750 (1932).
[9]K. I. Sixtus and L. Tonks, Phys. Rev. **37**, 1931 (1931).
[10]G. S. Krinchik and M. V. Chetkin, Usp. Fiz. Nauk **98**, 3 (1969) [Sov. Phys. Usp. **12**, 307 (1969)].
[11]V. G. Bar'yakhtar, V. V. Gann, Yu. I. Gorobets, G. A. Smolenskiĭ, and B. N. Filippov, Usp. Fiz. Nauk **121**, 593 (1977) [Sov. Phys. Usp. **20**, 298 (1977)].
[12]A. P. Malozemoff and J. C. Slonczewski, Magnetic Domain Walls in Bubble Materials, Academic Press, N. Y., 1979 (Russ. Transl., Mir, M., 1982).
[13]V. E. Zakharov, S. V. Manakov, S. P. Novikov, and L. P. Pitaevskiĭ, Teoriya solitonov (Soliton theory), Nauka, M., 1980.
[14]A. M. Kosevich, B. A. Ivanov, and A. S. Kovalev, Nelineĭnye volny namagnichennosti, Dinamicheskie i topologicheskie solitony (Nonlinear MagnetizationWaves. Dynamical and Topological Solitons), Naukova Dumka, Kiev, 1983.
[15]I. E. Dzyaloshinskiĭ, Zh. Eksp. Teor. Fiz. **32**, 1547 (1957) [Sov. Phys. JETP **5**, 1259 (1957)].
[16]E. A. Turov, Fizicheskie svoĭstva magnitouporyadochennykh kristallov, Izd. AN SSSR, Moscow, 1963 (Engl. Transl., Physical Properties of Magnetically Ordered Crystals, Academic Press, N. Y., 1965].
[17]A. I. Akhiezer, V. G. Bar'yakhtar, and S. V. Peletminskiĭ, Spinovye volny, Nauka, M., 1967 (Engl. Transl., Spin Waves, Wiley, N. Y., 1968).
[18]L. D. Landau and E. M. Lifshitz, Élektrodinamika sploshnykh sred, Nauka, M., 1982 [Engl. Transl. of earlier ed., (Electrodynamics of Continuous Media), Pergamon, Oxford, 1960].
[19]B. A. Ivanov and A. L. Sukstanskiĭ, Zh. Eksp. Teor. Fiz. **84**, 370 (1983) [Sov. Phys. JETP **57**, 214 (1983)].
[20]L. Walker, unpublished, cited in: Magnetism, Vol. 3 (ed. by G. Rado and H. Suhl), Pergamon, N. Y., 1963.
[21]E. Schlömann, J. Appl. Phys. **47**, 1142 (1976).
[22]R. Laudise and R. Parker, Crystal Growth, North-Holland, Amsterdam, 1972 (Russ. Transl., Mir, M., 1974).
[23]E. Kolb, D. L. Wood, and R. A. Laudis, J. Appl. Phys. **39**, 1362 (1968).
[24]S. A. Medvedev, A. M. Balbashov, and A. Ya. Chervonenkis, in: Monokristally tugoplavkikh i redkikh metallov (Single Crystals of Refractory and Rare Metals), Nauka, M., 1969, p. 27.
[25]K.P. Belov, A.K. Zvezdin, A. M. Kadomtseva, and R. Z. Levitin, Orientatsionnye perekhody v redkozemel'nykh magnetikakh (Orientational Transitions in the Rare-Earth Magnetic Materials), Nauka, M., 1979.
[26]R. L. White, J. Appl. Phys. **40**, 1061 (1969).
[27]V. G. Bar'yakhtar, B. A. Ivanov, and A. L. Sukstanskiĭ, Zh. Eksp. Teor. Fiz. **78**, 1509 (19980) [Sov. Phys. JETP **51**, 757 (1980)].
[28]B. A. Ivanov and V. P. Krasnov, Fiz. Tverd. Tela (Leningrad) **16**, 2971 (1974) [Sov. Phys. Solid State **16**, 1922 (1975)].
[29]L. N. Bulaevskiĭ and V. L. Ginsburg, Pis'ma, Zh. Eksp. Teor. Fiz. **11**, 404 (1970) [JETP Lett. **11**, 272 (1970)]; M. M. Farztdinov, S. D. Mal'ginova, and A. A. Khalfina, Izv. Akad. Nauk SSSR Ser. Fiz. **34**, 1104 (1970) [Bull. Acad. Sci., USSR Phys. Ser. **34**, 986 (1970)].
[30]G. E. Volovik and V. P. Mineev, Zh. Eksp. Teor. Fiz. **72**, 2257 (1977) [Sov. Phys. JETP **45**, 1186 (1977)].
[31]I. V. Bar'yakhtar and B. A. Ivanov, Fiz. Nizk. Temp. **5**, 759 (1979) [Sov. J. Low Temp. Phys. **5**, 361 (1979)]; Preprint No. 80-4, Physico-Technical Institute of the Academy of Sciences of the Ukrainian SSR, Donets, 1980.
[32]A. V. Zalesskiĭ, A. M. Savvinov, I. S. Zheludev, and A. N. Ivashchenko, Zh. Eksp. Teor. Fiz. **68**, 1449 (1975) [Sov. Phys. JETP **41**, 723 (1975)].
[33]C. S. Porter and E. G. Spencer, J. Appl. Phys. **29**, 485 (1958).
[34]D. L. Wood, L. M. Holmes, and J. P. Remeika, Phys. Rev. **185**, 689 (1969).
[35]B. T. Smith, J. Yamamoto, and E. E. Bell, J. Opt. Soc. Am. **65**, 605 (1975).
[36]A. F. Konstantinova, N. E. Ivanov, and B. N. Grechushnikov, Kristallografiya **14**, 283 (1969) [Sov. Phys. Crystallogr. **14**, 222 (1969)].
[37]W. J. Tabor and F. S. Chen, J. Appl. Phys. **40**, 2760 (1969).
[38]M. V. Chetkin and Yu. I. Shcherbakov, Fiz. Tverd. Tela (Leningrad) **11**, 1620 (1969) [Sov. Phys. Solid State **11**, 1314 (1969)].
[39]W. J. Tabor, A. W. Anderson, and L. G. Van Utert, J. Appl. Phys. **41**, 3018 (1970).
[40]M. V. Chetkin, Yu. I. Shcherbakov, and A. Ya. Chervonenkis, Izv. Akad. Nauk SSSR Ser. Fiz. **34**, 1041 (1970) [Bull Acad. Sci. USSR Phys. Ser. **34**, 929 (1970)].
[41]F. J. Kahn, P. S. Pershan, and J. P. Remeika, Phys. Rev. **186**, 891 (1969).
[42]R. V. Pisarev, Zh. Eksp. Teor. Fiz. **58**, 1421 (1970) [Sov. Phys. JETP **31**, 761 (1970)].
[43]M. V. Chetkin, Yu. S. Didosyan, A. I. Akhutkina, and A. Ya. Chervonenkis, Pis'ma Zh. Eksp,. Teor. Fiz. **12**, 519 (1970) [JETP Lett. **12**, 363 (1970)].
[44]M. V. Chetkin, Yu. S. Didosyan, and A. I. Akhutkina, Fiz. Tverd. Tela (Leningrad) **13**, 3414 (1971) [Sov. Phys. Solid State **13**, 2871 (1972)].
[45]M. V. Chetkin, Yu. S. Didosjan, and A. J. Akhutkina, IEEE Transl. Magn. **MAG-7**, 401 (1971).
[46]A. J. Kurtzig and W. J. Shockley, J. Appl. Phys. **39**, 5619 (1968).
[47]M. V. Chetkin and Yu. S. Didosyan, Fiz. Tverd. Tela (Leningrad) **15**, 1247 (1973) [Sov. Phys. Solid State **15**, 840 (1972)].
[48]M. V. Chetkin and Yu. S. Didosjan, Lasers Opt. Non-Conv. **44**, 12 (1973).

[49]R. S. Mezrich, IEEE Trans. Magn. **MAG-6**, 537 (1970).
[50]H. M. Haskal, *ibid.*, p. 542.
[51]C. H. Tsang and R. L. White, AIP Conf. Proc. **24**, 749 (1975).
[52]C. H. Tsang, R. L. White, and R. M. White, *ibid.*, **29**, 552 (1976).
[53]a) C. H. Tsang, R. L. White, and R. M. White, J. Appl. Phys. **49**, 6052 (1978). b) C. H. Tsang and R. L. White, *ibid.*, p. 6062.
[54]A. H. Bobek, in: Ferrites: Proc. Intern. Conf., Tokyo, publ. by Univ. Tokyo Press, 1971, p. 361.
[55]A. H. Bobek and E. Della Torre, Magnetic Bubbles, North-Holland, Amsterdam, 1975 (Russ. Transl., Énergiya, M., 1977).
[56]H. Callen and R. M. Josephs, J. Appl. Phys. **42**, 1977 (1971).
[57]F. B. Humphrey, IEEE Trans. Magn. **MAG-11**, 1679 (1975).
[58]S. Konishi, T. Kawamoto, and M. Wada, IEEE Trans. Magn. **MAG-10**, 642 (1974).
[59]S. Konishi, T. Miyama, and K. Ikeda, Appl. Phys. Lett. **22**, 258 (1975).
[60]E. W. Lee and D. R. Callaby, Nature **182**, 254 (1958).
[61]M. V. Chetkin, A. N. Shalygin, and A. de la Campa, a) Fiz. Tverd. Tela (Leningrad) **19**, 3470 (1977) [Sov. Phys. Solid State **19**, 2029 (1977)]; b) Prib. Tekh. Eksp. No. 1, 207 (1980) [Instrum. Exp. Tech. **23**, 215 (1980)].
[62]M. V. Chetkin and A. de la Campa, Pis'ma Zh. Eksp. Teor. Fiz. **27**, 168 (1978) [JETP Lett. **27**, 157 (1978)].
[63]M. V. Chetkin and A. I. Akhutkina, Zh. Eksp. Teor. Fiz. **78**, 761 (1980) [Sov. Phys. JETP **51**, 383 (1980)].
[64]M. V. Chetkin, A. I. Akhutkina, N. N. Ermilova, A. P. Kuz'menko, and Yu. S. Didosyan, Zh. Eksp. Teor. Fiz. **81**, 2206 (1981) [Sov. Phys. JETP **54**, 1172 (1981)].
[65]M. H. Kryder and F. B. Humphrey, J. Appl. Phys. **47**, 2469 (1976).
[66]F. B. Humphrey, IEEE Transl. Mgn. **MAG-11**, 1679 (1975).
[67]G. P. Vella-Coleiro, J. Appl. Phys. **47**, 3287 (1976).
[68]G. P. Vella-Coleiro and T. I. Nelson, Appl.Phys. Lett. **24**, 397 (1974).
[69]V. N. Dudorov, V. V. Randoshkin, and R. V. Telesnin, Usp. Fiz. Nauk **122**, 253 (1977) [Sov. Phys. Usp. **20**, 505 (1977)].
[70]L. P. Ivanov, A. S. Logginov, V. V. Randoshkin, and R. V. Telesnin, Pis'ma Zh. Eksp. Teor. Fiz. **23**, 627 (1977) [JETP Lett. **23**, 575 (1976)].
[71]F. C. Rossol, J. Appl. Phys. **40**, 1082 (1969).
[72]T. Ikuta and R. Shimizu, J. Phys. D 7, 726 (1974).
[73]M. V. Chetkin, Zh. I. Bynzarov, S. N. Gadetskiĭ, and Yu. I. Shcherbakov, Zh. Eksp. Teor. Fiz. **81**, 1898 (1981) [Sov. Phys. JETP **54**, 1005 (1981)].
[74]M. V. Chetkin, S. N. Gadetskiĭ, and A. I. Akhutkina, Pis'ma Zh. Eksp. Teor. Fiz. **35**, 373 (1982) [JETP Lett. **35**, 459 (1982)].
[75]M. V. Chetkin, A. I. Akhutkina, and A. P. Kuzmenko, J. Appl. Phys. **53**, 7864 (1982).
[76]M. V. Chetkin, A. P. Kuz'menko, S. N. Gadetskiĭ, V. N. Filatov, and A. I. Akhutkina, Pis'ma Zh. Eksp. Teor. Fiz. **37**, 223 (1983) [JETP Lett. **37**, 264 (1983)].
[77]M. V. Chetkin, A. P. Gadetskiĭ, A. P. Kuz'menko, and A.I. Akhutkina, Zh. Eksp. Teor. Fiz. **86**, 1411 (1984) [Sov. Phys. JETP **59**, 825 (1984)]; M. V. Chetkin, S. N. Gadetskiĭ, A. P. Kuz'menko, and V. N. Filatov, Prib. Tekh. Eksp. No. 3 196 (1984) [Instrum. Exp. Tech. **27**, 740 (1984)].
[78]I. O. Shipmann, Appl. Phys. Lett. **10**, 3 (1967).
[79]F. C. Rossol, Phys. Rev. Lett. **24**, 1021 (1970).
[80]A. V. Zalesskiĭ, V. G. Krivenko, and A. M. Balbashov, Fiz. Tverd. Tela (Leningrad) **23**, 3459 (1981) [Sov. Phys. Solid State **23**, 2011 (1981)].
[81]H. L. Huang, Phys. Rev. Lett. **29**, 432 (1972).
[82]R. W. Shumate, J. Appl. Phys. **42**, 5770 (1971).
[83]A. Rosencwaig, J. Appl. Phys. **42**, 5773 (1971).
[64]E. M. Gyorgy and F. B. Hagedorn, J. Appl. Phys. **39**, 88 (1968).
[85]F. B. Hagedorn, AIP Conf. Proc. **5**, 72 (1972).
[86]A. N. Grishmanovskiĭ, V. V. Lemanov, G. A.Smolenskiĭ, A. M. Balbashov, and A. Ya. Chervonenkis, Fiz. Tverd. Tela (Leningrad) **16**, 1426 (1974) [Sov. Phys. Solid State **16**, 916 (1974)].
[87]G. Gorodetsky and B. Luthi, Phys. Rev. **82**, 3688 (1974).
[88]V. G. Bar'yakhtar, B. A. Ivanov, and A. L. Sukstanskiĭ, Pis'ma Zh. Eksp. Teor. Fiz. **27**, 226 (1978) [JETP Lett. **27**, 211 (1978)].
[89]V. G. Bar'yakhtar, B. A. Ivanov, and A. L. Sukstanskiĭ, Pis'ma Zh. Tekh. Fiz. **5**, 853 (1979) [Sov. Tech. Phys. Lett. **5**, 351 (1979)]; Zh. Eksp. Teor. Fiz. **78**, 1509 (1980) [Sov. Phys. JETP **51**, 757 (1980)].
[90]A. K. Zvezdin, Pis'ma Zh. Eksp. Teor. Fiz. **29**, 605 (1979) [JETP Lett. **29**, 553 (1979)].
[91]V. M. Eleonskiĭ, N. N. Kirova, and N. E. Kulagin, Zh. Eksp. Teor. Fiz. **79**, 321 (1980); **80**, 357 (1981) [Sov. Phys. JETP **52**, 162 (1980); **53**, 182 (1981)].
[92]P. D. Kim and D. Ch. Khvan, Fiz. Tverd. Tela (Leningrad) **24**, 2300 (1982) [Sov. Phys. Solid State **24**, 1306 (1982)]; V. G. Bar'yakhtar, B. A. Ivanov, P. D.Kim, A. L. Sukstanskiĭ, and D. Ch. Khvan, in: Tezisy Vsesoyuznoĭ konferentsii po fizike magnitnykh yavleniĭ (Abstracts of Papers Presented at the All-Union Conference on the Physics of Magnetic Phenomena), Tula, 1983, Vol. 2, p. 60.
[93]M. V. Chetkin, Yu. I. Shcherbakov, S. N. Gadetskiĭ, and V. D. Tereshchenko, Preprint No. 10/1984, Physics Department, Moscow State University, Moscow, 1984; Zh. Tekh. Fiz. **55**, 207 (1985) [Sov. Phys. Tech. Phys. **30**, 120 (1985)].
[94]W. Jantz, J. R. Sandercock, and W. Wettling, J. Phys. C **9**, 2229 (1976).
[95]A. F. Andreev and V. I. Marchenko, Usp. Fiz. Nauk **130**, 39 (1980) [Sov. Phys. Usp. **23**, 21 (1980)].
[96]M. I. Kaganov and V. M. Tsukernik, Zh. Eksp. Teor. Fiz. **34**, 106 (1958) [Sov. Phys. JETP **7**, 73 (1958)]; E. A. Turov and Yu. P. Irkhin, Izv. Akad. Nauk SSSR Ser. Fiz. **22**, 1168 (1958).
[97]N. N. Bogolyubov and S. V. Tyablikov, Zh. Eksp. Teor. Fiz. **19**, 251 (1949).
[98]A. S. Borovik-Romanov, in: Antiferromagnetizm: Itogi nauki (Antiferromagnetism: Results of Science), Vol. 4, VINITI, Moscow, 1962, p. 7.
[99]A. S. Borovik, Romanov and N. M. Kreines, Phys. Rep. **81**, 351 (1982).
[100]R. M. White, R. J. Nemanich, and C. Herring, Phys. Rev. B **25**, 1822 (1982).
[101]G. A. Kraftmakher, V. V. Meriakri, A. Ya. Chervonenkis, and V. I. Shcheglov, Zh. Eksp. Teor. Fiz. **63**, 1353 (1972) [Sov. Phys. JETP **36**, 714 (1973)].
[102]A. S. Abysov and B. A. Ivanov, Zh. Eksp. Teor. Fiz. **76**, 1700 (1979) [Sov. Phys. JETP **49**, 865 (1979)].
[103]A. V. Zuev and B. A. Ivanov, Fiz. Tverd. Tela (Leningrad) **22**, 3 (1980) [Sov. Phys. Solid State **22**, 1 (1980)].
[104]V. G. Bar'yakhtar, I. V. Bar'yakhtar, B. A. Ivanov, and A. L. Sukstansky, Preprint No. ITP-82-166E, Institute of Theoretical Physics, Academy of Sciences of the Ukrainian SSR, Kiev, 1983.
[105]I. V. Bar'yakhtar and B. A. Ivanov, Preprint No. ITF-83-111R, Institute of Theoretical Physics, Academy of Sciences of the Ukrainian SSR, Kiev, 1983.
[106]V. G. Bar'yakhtar, *in*: Problemy sovremennoĭ teoreticheskoĭ fiziki (Problems of Contemporary Theoretical Physics), Naukova Dumka, Kiev, 1983, p. 57; Zh. Eksp. Teor. Fiz. **87**, 1501 (1984) [Sov. Phys. JETP **60**, 863 (1984)].
[107]M. V. Chetkin, A. I. Akhutkina, N. N. Ermilova, and D. I. Kondratyuk, Fiz. Tverd. Tela (Leningrad) **22**, 1849 (1980) [Sov. Phys. Solid State **22**, 1075 (1980)].
[108]A. V. Zuev, B. A. Ivanov, and A. L. Sukstanskiĭ, Fiz. Nizk. Temp. **8**, 1190 (1982) [Sov. J. Low Temp. Phys. **8**, 603 (1982)].
[109]A. V. Zuev and B. A. Ivanov, Zh. Eksp. Teor. Fiz. **82**, 1679 (1982) [Sov. Phys. JETP **55**, 971 (1982)].
[110]V. G. Bar'yakhtar, B. A. Ivanov, and A. L. Sukstanskiĭ, Zh. Eksp. Teor. Fiz. **75**, 2180 (1978) [Sov. Phys. JETP **48**, 1098 (1978)].
[111]A. K. Zvesdin and A. F. Popkov, Fiz. Tverd. Tela (Leningrad) **21**, 1334 (1979) [Sov. Phys. Solid State **21**, 771 (1979)].
[112]V. G. Bar'yakhtar and B. A. Ivanov, Pis'ma Zh. Eksp. Teor. Fiz. **35**, 85 (1982) [JETP Lett. **35**, 101 (1982)].
[113]B. A. Ivanov, V. F. Lapchenko, and A. L. Sukstanskiĭ, Fiz. Tverd. Tela (Leningrad) **25**, 3061 (1983) [Sov. Phys. Solid State **25**, 1766 (1983)].
[114]V. G. Bar'yakhtar, B. A. Ivanov, P. D. Kim, A. L. Sukstanskiĭ, and D. Ch. Khvan, Pis'ma Zh. Eksp. Teor. Fiz. **37**, 35 (1983) [JETP Lett. **37**, 41 (1983)].
[115]I. V. Bar'yakhtar, B. A. Ivanov, and A. L. Sukstanskiĭ, Pis'ma Zh. Tekh. Fiz. **6**, 1497 (1980) [Sov. Tech. Phys. Lett. **6**, 645 (1980)].
[116]A. A.Abrikosov, L. P. Gor'kov, and I. E. Dzyaloshinskiĭ, Metody kvantovoĭ teorii polya v statisticheskoĭ fiziki, Fizmatgiz, M., 1962 (Engl. Transl., Methods of Quantum Field Theory in Statistical Physics, Prentice-Hall, Englewood Cliffs, N. J., 1963); A. I. Akhiezer and S. V. Peletminskiĭ, Metody statisticheskoĭ fiziki, Nauka, M., 1977 (Engl. Transl., Methods of Statistical Physics, Pergamon, New York, 1981)
[117]A. K. Zvezdin, A. A. Mukhin, and A. F. Popkov, Preprint No. 108, P. N. Lebedev Physics Institute, Academy of Sciences of the USSR, Moscow, 1982.
[118]A. A. Andronov, A. A.Vitt, and S. É. Khaĭkin, Teoriya kolebaniĭ, Fizmatgiz, M., 1995 (Engl. Transl., Theory of Oscillators, Addison-Wesley, Reading, Mass., 1966).
[119]V. G. Bar'yakhtar and B. A. Ivanov, Fiz. Met. Metalloved. **36**, 690 (1973).
[120]W. V. Chetkin, S. N. Gadetsky, V. N. Filatov, A. P. Kuzmenko, and A.

V. Kiryushin, in: Intermag—1983—Philadelphia, 1983, EB-8.
[121]T. Suzuki, L. Gal, and E. Maekewa, Jpn. J. Appl.Phys. **19**, 627 (1980); A. S. Logginov and G. A. Nepokoĭchitskiĭ, Pis'ma Zh. Eksp. Teor. Fiz. **35**, 22 (1982) [JETP Lett. **35**, 27 (1982)]. L. P. Ivanov, A. S. Logginov, and G. A. Nepokoĭchitskiĭ, Zh. Eksp. Teor. Fiz. **84**, 1006 (1983) [Sov. Phys. JETP **57**, 583 (1983)].
[122]M. V. Chetkin and S. N. Gadetskiĭ, Pis'ma Zh. Eksp. Teor. Fiz. **38**, 260 (1983) [JETP Lett. **38**, 308 (1983)].
[123]B. A. Ivanov and G. K. Oksyuk, Preprint No. ITF-84-8R, Institute of Theoretical Physics of the Academy of Sciences of the Ukrainian SSR, Kiev, 1984.
[124]A. K. Zvezdin and A. F. Popkov, Pis'ma Zh. Tekh. Fiz. **10**, 449 (1984) [Sov. Tech. Phys. Lett. **10**, 188 (1984)].
[125]A. L. Sukstanskiĭ, Zh. Tekh. Fiz. **54**, 1204 (1984) [Sov. Phys. Tech. Phys. **29**, 689 (1984)].

Translated by A. K. Agyei